5-20-2005

Investigations of Pile Foundations in Brownfields

Ranjan Satyamurthy
University of New Orleans

INVESTIGATIONS OF PILE FOUNDATIONS IN BROWNFIELDS

A Thesis

Submitted to the Graduate Faculty of the
University of New Orleans
in partial fulfillment of the
requirements for the degree of

Master of Science
in
The Department of Civil and Environmental Engineering

by

Ranjan Satyamurthy

B.E., Visveswaraiah Technological University, 2003

May, 2005

DEDICATION

To my parents,

with respect, love and gratitude.

"Maatru Devo Bhava,

Pitru Devo Bhava,

Acharya Devo Bhava,

Atithi Devo Bhava"

"Mother is divine,

Father is divine,

Teacher is divine,

Guest is divine’.

ACKNOWLEDGEMENTS

The thesis and my graduate studies are greatly indebted to Dr. Mysore S Nataraj. His erudition, patience, encouragement and passion for perfection have been a great source of inspiration. His faith and trust in my abilities and continuous support has been the cornerstone of my studies at UNO. His patience, advice and guidance are acknowledged with gratitude. There is nothing more important than the knowledge that comes to an individual by a teacher; I am blessed indeed to have him as my mentor. Dr.Nataraj is the greatest influence in my life and career.

I would like to express my sincere gratitude to Dr. Kenneth L. McManis for his guidance, support and deep insight into the project. His technical suggestions and patience with the review of my thesis is appreciated.

Special thanks are reserved for Dr. Gordon P Boutwell. Every meeting with Dr.Boutwell has enriched my knowledge and understanding of the investigation. His continuous support and review of my work is deeply appreciated. He has been a source of inspiration, strength and will be a role model forever.

I wish to express my thanks to Dr.Donald Barbe` for his support, encouragement and patience with the review of my thesis.

Sincere and heartfelt thanks are due to my special friend Mr. Byron C Landry, for his assistance with all phases of the model tests. He was always present to help me during the experimental work related to this project.

The patience and technical assistance of Mr. Frank Sebro and Mr. Aniruddha Dasgupta during the course of this project are highly appreciated.

I would like to thank Mr. Hugh L. Till of the Tangipahoa Parish Regional Solid Waste Facility for supplying the clay used in the model test chambers.

I would like to thank my friends Dr.Bogdan Barbu, Mr. Ramesh Karuppusamy, Dr. Ricardo de Abreu, Mr. Sanjay Datar, Mr. Sreekant Pagadala, and others for their help, suggestions and support. Thanks are due to all my other friends and graduate students of Civil and Environmental Engineering department for their support.

Thanks are due to Ms. Juana Villavaso, for her help.

I gratefully acknowledge the contributions of the professors at S.J.College of Engineering, India for preparing me for graduate studies, with special thanks to Dr. Sundarraj Krishna Prasad, my mentor during my undergraduate studies.

Finally, I want to thank my beloved parents and my elder brother, for their love, support and encouragement. Above all I would like to thank God for blessing me with everything.

TABLE OF CONTENTS

LIST OF TABLES

LIST OF FIGURES

ABSTRACT

"Brownfields" are real estate property with subsurface or surface contamination. The redevelopment of Brownfields is required to clean, improve and protect the environment. Piles foundations are often used in Brownfields to support structures. Regulators are concerned about the environmental safety of pile foundations in Brownfields sites.

Piling in Brownfields may lead to transport of contaminants from the contaminated region to the underground aquifers. The purpose of this investigation is to determine the potential for contaminant transport due to pile foundation in Brownfields.

This investigation is an extension of previous research conducted at the University of New Orleans and ascertains the potential for contaminant transport from concrete piles of different shape, depth of penetration and method of installation.

The results of large scale model tests and Finite Element studies are presented. The investigation indicates the possibility of contamination only in selected cases of piles.

1. INTRODUCTION

In the smallest towns and the largest cities, empty warehouses, decrepit factories, and junk-filled lots are constant reminders of how quickly a source of community pride can become a dangerous, unsightly, and unwanted burden. Such sites are termed Brownfields and are defined as real estate property, the expansion, redevelopment or reuse of which may be complicated by the presence or potential presence of a hazardous substance, pollutant or contaminant (US EPA, 2002). The blight and negative economic impact of abandoned, underused, and potentially contaminated properties is seen throughout the United States and in most parts of the world. According to the US Environmental Protection Agency (US EPA, 2003) the number of brownfields across the United States range from 450,000 to as many as a million.

Cleaning up and redevelopment of brownfields is required in order to reduce the pressure for development of undeveloped open land and to improve and protect the environment (US EPA, 2003). Redevelopment of brownfields includes building on brownfield sites. In many instances, subsurface characteristics, superstructure loads, settlement criteria and structural safety considerations limit the use of shallow foundations. Deep foundations (piles) become necessary in such circumstances.

By definition, brownfields have surface and near surface contamination. Piling on brownfields sites often leads to piles penetrating the contaminated zone. The pile may then fully penetrate an underlying aquitard, possibly entering a deeper underlying aquifer. The installation process of the pile, the pile material, depth of penetration, the shape of the pile and other factors may potentially cause the migration of contaminant into the aquifer from the near surface contaminated zone.

Regulators are concerned about piling in contaminated sites and the potential risks involved. The regulatory concerns and design requirements needed to satisfy these concerns are expensive and complicated.

There is a strong need to investigate the potential for contaminant transport due to piles, and to determine suitable mitigation measures.

2. LITERATURE REVIEW

Piling in contaminated sites represents a potential threat for groundwater contamination. A comprehensive literature survey provided very few publications that address this problem. Concerns about the existence of vertical migration have been proved true by two investigations. Hayman et al., (1993) conducted benchmark model tests of pile foundations penetrating an aquitard "sandwiched" between aquifers. The model tests investigated circular steel and wooden dowel piles. The model tests were made to observe potential avenues of contaminant transport in conjunction with pile foundations. Their investigation concluded that piles driven through shallow contaminated strata to a deep water bearing strata will carry down a finite quantity of contamination and the pile-soil contact does not necessarily provide a conduit for vertical contaminant migration. A groundwater contamination investigation and a remedial action program at a major chemical plant were conducted by Campbell et al., 1984. The existence of a downgradient which allowed contaminant migration was observed in wells at the site. The migration of contaminants in conjunction with piles was not the main objective for this investigation, the existence of a downgradient that allowed contaminant migration in wells was proved true during the test.

Dunn (1995) discussing various aspects of design and construction of foundations at landfills mentions that "….. related to water quality, a basic policy has emerged that the installation of pile foundations cannot increase the potential for migration of contaminants from the MSW to groundwater underlying a landfill," although no justification was provided. Further, the author suggests that for sites underlain with soft clays, the pile driving and installation process must demonstrate to the regulators that a seal will be maintained around the pile during and after driving through the sealing layer.

Among the available literature the investigation by Boutwell et al., (2000) focused solely on this phenomenon. The study considered mechanisms of contaminant transfer and the influence of pile type and material. The mechanisms suggested include: direct transfer of contaminated soil by the pile tips, formation of a preferential pathway by the pile, flow through pile material itself, and use of chemically treated piles.

The direct transfer part was found to be minimal, especially with pointed pile tips. The pathway part was investigated using model studies in a chamber in which flow was induced through clay columns with segmented bases to separate different regions of flow. Models with and without various types of model piles fully penetrating the clay were permeated with water and brine. Both flow and contaminant measurements indicated no increase in transmission rates for displacement type piles of low-permeability materials, i.e., treated wood and steel pipe piles. Two piles were found to induce high pollutant transmission, untreated wood by internal flow and steel "H" piles by pathway formation (due to low lateral pressures). They concluded that piles of the proper types driven through a contaminated zone did not create a significant pollution potential. The study advanced the understanding of the potential of contaminant transport through piles. Additional details are given in chapter 4.

The Environmental Agency of United Kingdom, (Environmental Agency, 2001) has published guidance on pollution prevention during piling and ground improvements methods. This publication has referenced the works of Hayman et al., (1993) and Boutwell et al., (2000). The publication has provided a summary guidance on pollution prevention associated with piling in contaminated sites.

Kamon et al., (2005) investigated interface transmissivity caused by piles penetrating a clay layer.

Their study was to evaluate the integrity of the bottom clay layer at a landfill site if piles were installed through the clay layer. Simple experiments with rigid wall and flexible wall permeameters were used to determine the interface transmissivity between the clay and steel. They suggest that if the clay is deformable enough to seal the interface between the clay and the pile due to lateral pressure, the interface leakage becomes negligible. A clay layer which has already consolidated may not provide this. From their experiments they found the interface leakage to be very low. They recommend that, while installing piling through landfill liners, the barrier performance should be evaluated based on hydraulic conductivity, thickness and state of consolidation of the layer.

The studies by Boutwell et al., (2000) and McManis et al., (2002) form the precursor to the present investigation. The role of pile material and pile type on potential contaminant transport was evaluated. The salient aspects of this earlier study are described in the Chapter 4 "Methodology of Investigations," and the results are summarized in other chapters.

3. OBJECTIVE AND SCOPE OF THE STUDY

The objective of this study is to ascertain the possible causes of potential contaminant transfer by conducting model tests involving various piles and performing numerical studies. The scope of this investigation focuses on the effect of shape, installation procedure and the depth of penetration of concrete piles on potential contaminant transport. The model test results and the numerical studies will throw light upon some aspects of potential contaminant transport which may occur when pile foundations are used in brownfields.

This study is concerned with the influence, if any of the following factors:

3.1 Shape of the Pile

The pile shape may have a potential impact on pollutant transport. Square and circular model piles are utilized to determine the influence, if any, of the pile shape on potential contaminant transport. The model concrete piles used for the tests had constant cross-sections and flat tips.

3.2 Depth of Penetration

The quality of soils usually improves with depth. Thus, the bearing capacity of a pile generally increases with the depth of penetration. The depth of penetration of piles may have an effect on the potential contaminant transport. In regions where the subsurface is stratified into alternate aquifers and confining strata (such as aquiclude or aquitard), driving the pile into the aquifer provides high end-bearing capacity.

The economic benefits of driving a pile fully into the bottom aquifer can be demonstrated by the following example; a 1 ft diameter pile driven 95.00 ft (28.95 m) into normally consolidated

clay has half the total capacity of a similar pile driven 5.00 ft (1.52 m) further into the aquifer (dense sand) (Boutwell et al., 2005).

Fully penetrating piles and partially penetrating piles were studied for the effects that they had on potential contaminant transport.

3.3 Method of Installation

The method of installation may significantly influence the potential for contaminant transport. Piles are classified based on their installation methods as “driven” (typically “displacement piles”) and “bored” or “non displacement piles”.

In driven piles, the pile is driven into the soil vertically without removal of the soil to the ground surface. H-piles are small displacement piles as they displace a relative small quantity soil as they are driven. A close ended circular pile or a square pile having a flat tip can be regarded as a large displacement pile because they displace a large volume of soil (Das B.M., 1999 and Coduto., 2001).

In bored piles, a core of the soil is extracted and replaced with the pile, typically formed by casting concrete in-situ. Displacement of surrounding soil is minimized. Placement of bored piles causes very little change in the state of stress in the soil. Concrete driven piles and cast-in-place piles were used in this study.

4. METHODOLOGY OF INVESTIGATION

A study by Boutwell et al., (2000) initiated the UNO experimental investigation related to pile foundations in brownfields. This present study continues the study and forms the second phase of the UNO investigation. In order to establish a basis for experimental investigations, Boutwell et al., (2000) considered different mechanisms for contaminant transfer. These are described in the following paragraphs, followed by the details of setting up and conducting model tests.

4.1 Potential for Contamination

Boutwell et al., (2001) have identified four mechanisms for potential contaminant transfer. The first mechanism involves consideration for contaminant from the pile material itself, such as a creosoted timber pile. This scenario is limited in today's real-world construction, and was not studied. However, the mechanisms that apply to all piles are:

4.1.1 Direct Transfer

This potential mechanism is illustrated in Figure 1. Soil bearing capacity theory (Terzaghi, 1943) indicates that there is a roughly conical "dead zone" or plug of soil just below the pile tip. Under certain conditions, the plug could be created in the contaminated zone (Stage 1) and carried along with the pile tip (Stage 2) all the way vertically into the aquifer. This results in a one-time slug of contaminants reaching the aquifer (Stage 3). A plume of this contaminant can then be carried away from the pile tip by normal contaminant transport phenomena.

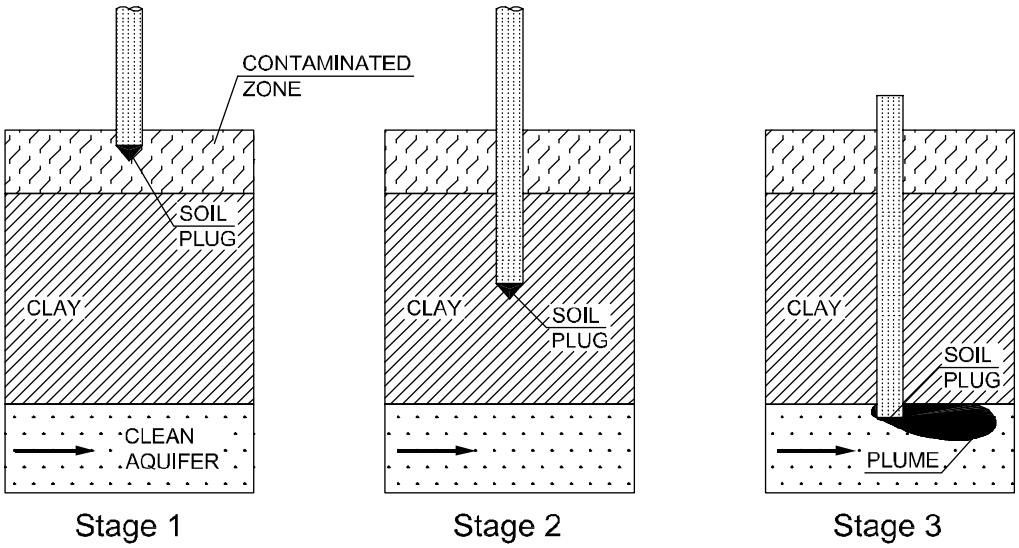

Figure 1 – Different stages of Direct Transfer (After Boutwell et al., (2001)).

4.1.2 Conduit Formation

Conduit formation represents a significant threat of contaminant transfer. The presence of an open annulus of 0.06 in (0.15 cm) around a 1 in (2.54 cm) pile will provides the same capacity of flow as a pile made of gravel (Boutwell et al, 2005). Thus, the formation of an open annuls will result in high flow rates and greater amount of contaminant transport by advection. This mechanism is presented in Figure 2 and represents a long term threat. The conduit is most likely to occur in the soil zone disturbed by pile-driving (around and along the pile/soil interface). Some of the favorable conditions for conduit formation include:

(1) the formation of an annular void or at least a zone of higher permeability, around or along the pile, and

(2) a downwards hydraulic gradient to cause flow, i.e., the groundwater head in the contaminated zone must be greater than that in the aquifer.

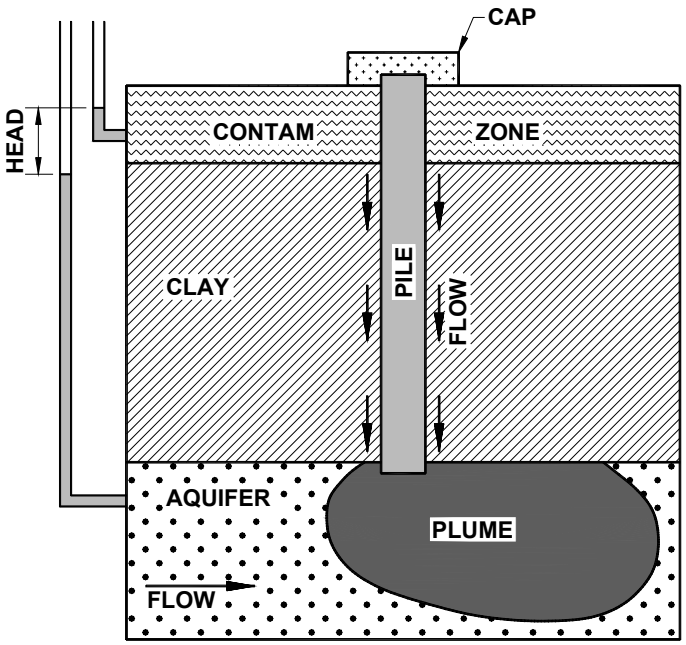

Figure 2 –Conduit formation flow along the pile/soil interface
(After Boutwell et al., (2001)).

4.1.3 Wicking

Wicking represents flow through the pile material. This is as shown in Figure 3. The permeability of the pile material relative to the surrounding soil indicates the potential for wicking. Wooden and some concrete piles are more permeable than the soil (usually clay) they are driven into. There is a potential for long term contaminant transport occurring by wicking in brownfields where a downgradient is producing flow through the pile.

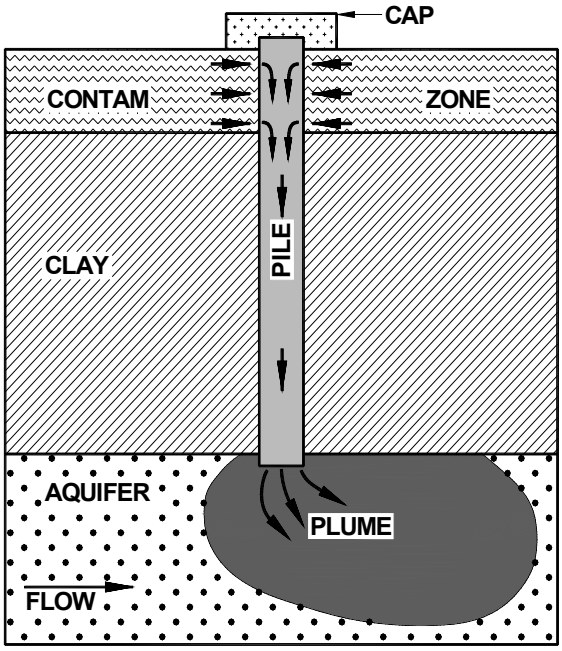

Figure3 – Flow through Pile Material (Wicking). (After Boutwell et al., (2001)).

4.1.4 Regulatory Response

Some regulatory authorities require "hydraulic isolation" of the pile from the contaminated zone. A typical such requirement is illustrated in Figure 4. The first step includes, drilling out the contaminated soils. Then, a casing (steel or plastic) is to be grouted in place, extending below the contaminated soils to prevent the contaminants from having access to the "disturbed" zone or pile. This is shown in Figure 4 as Steps 1, 2, and 3. Finally, the pile is to be driven through the casing (Step 4). Then, the casing must be grouted up (Step 5). This procedure is expensive and can easily cost as much as the pile.

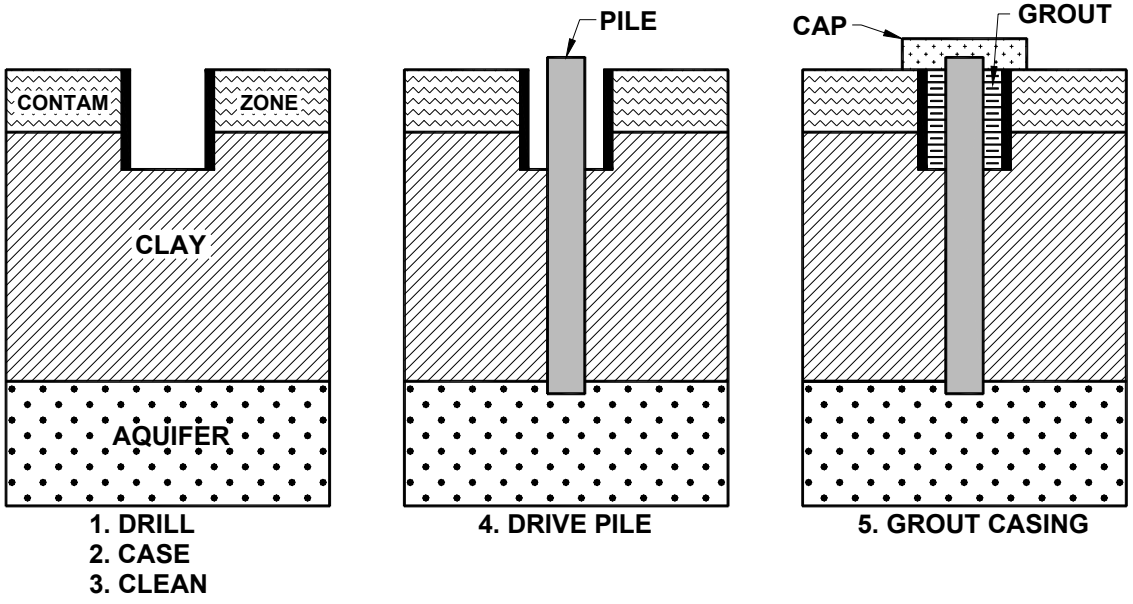

Figure 4 – Typical Regulatory Requirement (After Boutwell et al., (2001)).

An alternative would be to stop the piles in the clay. This leaves a protective clay barrier beneath the pile tip. Such partially penetrating piles may not pose significant threat of contaminant transport. Partial penetration results in reduction of the pile capacity, and necessitates the use of more piles and thus proves to be very expensive.

4.2 Test Set up.

The pile model tests for this study were conducted using a series of six cylindrical test chambers described in McManis et al., (2002). The test set up consists of six identical cylindrical chambers which were fabricated using PVC. Each test chamber is 12 in (30 cm) in diameter and 27 in (68 cm) in height. A schematic of the model test chamber is provided in Figure 5.

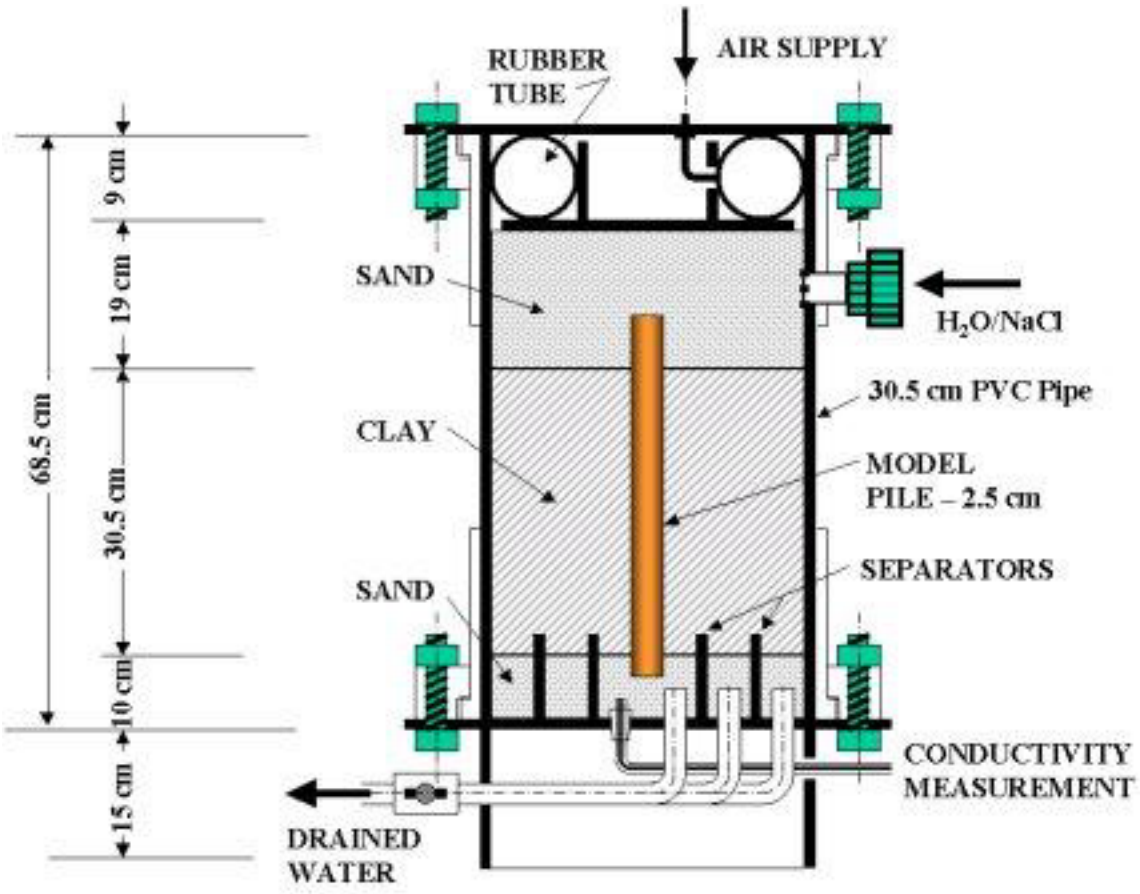

Figure 5. Schematic of the model test chamber (After Boutwell et al., 2000).

Each test chamber consists of three parts, the bottom plate, the middle section and the top plate. The bottom plate is a 19.00 in (48.26 cm) diameter PVC plate with two concentric PVC rings having diameters of 4.00 in (10.16 cm), and 8.00 in (20.32 cm) respectively, mounted on the upper side. The separator rings are shown in Figure 6, which is a photograph taken from the top of the chamber.

Figure 6. Photograph showing the center, middle and outer rings to separate the flow.

When the chamber is assembled, the lower part is filled with sand flush to the top surface of the separator rings. The separator rings separate the drainage of effluent, which flows out through the drain tubes. The drain tubes are connected to the bottom plate by holes drilled in the PVC plate. This separate collection is done to identify areas of high or low fluid migration. The inlets of the tubes are covered with 500 μm mesh to prevent sand intrusion and blocking of the drainage pipes. All the three regions are equipped with a conductivity probe (manufactured by Myron L Company) to measure electrical conductivity of the draining liquid. The conductivity probes are covered with metal gauze to prevent sand intrusion and are connected to a central control panel where the electrical conductivity measurements are recorded.

Figure 7 shows a bottom view from the base part with drainage pipes and conductivity probes mounted. The base part can be fastened to the trunk by means of 12 radially symmetric holes of 1.00 in (2.54 cm) diameter. The socket is made of a 12.00 in (30.48 cm) diameter and 6.00 in (15.24 cm) high PVC pipe. Holes are drilled on the side of the socket to accommodate drain tubes and conductivity wires. The socket is connected to the plate with metal elbows and screws to assure resistance to the weight of above chamber and soil

The middle section (trunk) is a 12.00 in (30.48 cm) diameter by 27.00 in (68.58 cm) high PVC pipe. It has a PVC flange on both ends for bolting the base section and the top cover plate. Fastening the connections at the top and the bottom renders an air-tight seal. After a test the parts can be unscrewed, cleaned and reassembled for another test.

A PVC adapter of size 0.50 in (1.27 cm) is mounted 6.50 inch (16.51 cm) from the top for the permeant supply. This adapter fits into a union of size 0.50 in (1.27 cm) placed to connect and disconnect the permeant supply easily. The permeant is supplied from a separate permeant chamber under pressure.

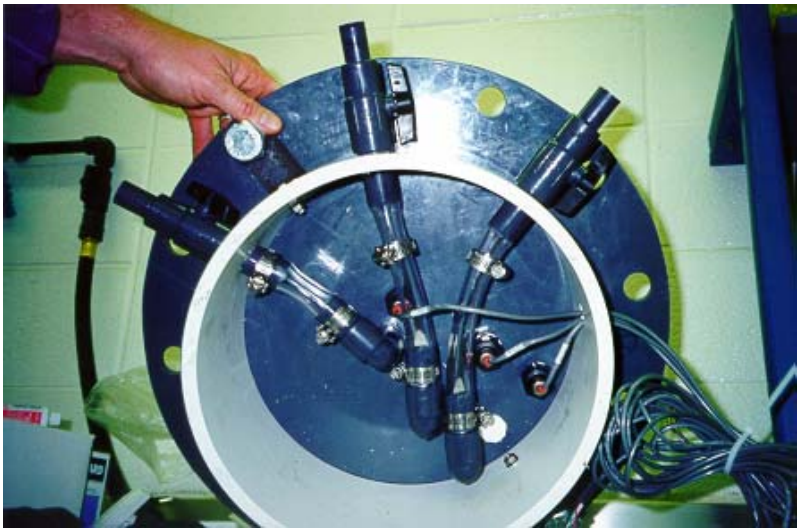

Figure 7. Base section of test chamber, bottom view

The top cover plate is a 19.00 in (48.26 cm) diameter PVC plate with 12 radial symmetric holes at the side. It is connected to the middle part with bolts. A bushing is placed eccentrically to provide air pressure to the rubber tube on the inside of the chamber. The air supply can be disconnected on the outside in order to move the chamber for emptying, cleaning and refilling. The air supply provides the air pressure required for inflating the tube. A 5.50 in (13.97 cm) diameter and 3.00 in (7.62 cm) high PVC pipe is glued at the inside of the top cover plate to keep the rubber tube centered.

The top plate is a 12.00 in (30.48 cm) diameter made out of PVC and is placed on top of the upper sand layer. To simulate overburden pressure a pressurized rubber tube is placed between the top plate and the top cover plate. By inflating the tube in this confined volume generates pressure, which then acts on the soil material and simulates overburden pressure. The height and diameter of the confining volume have to be about the same throughout the test since the relation between tube pressure and effective overburden pressure has been calibrated to a specific volume.

4.3 Test Procedure

Each test chamber is a 12.00 inch (30.48 cm) diameter PVC pipe 27.00 inches (68.58 cm) high with sand and clay layers placed to simulate the field conditions of a natural clay aquitard overlying a sand aquifer. The model pile is driven or cast-in-place in the clay and then flow induced from top to bottom.

The top sand layer is highly permeable and distributes the in-flowing “contaminated” permeant uniformly before it enters the clay.

The bottom sand layer allows collecting and draining the permeant exiting from the clay. As this layer is divided by three concentric rings; the flow can be collected separately. The conductivity meters are utilized to measure the salinity of the effluent.

4.4 Model Tests (First Phase)

The testing program by Boutwell et al., 2000 and McManis et al., 2003 involved a circular steel pile, a steel H-section pile, a treated wood pile, an untreated wood pile and a sand pile. The clay used for the tests was obtained from Tangipahoa Parish Regional Solid Waste Facility in Louisiana. The clay had a Liquid Limit of 34, Plastic Limit of 15 (ASTM D 4318). Figure 8 shows the grain size distribution of the sample based on Hydrometer analysis (ASTM D 422). It was compacted into the chamber in 5 layers to about 88% Standard Proctor Compaction (ASTM D698).

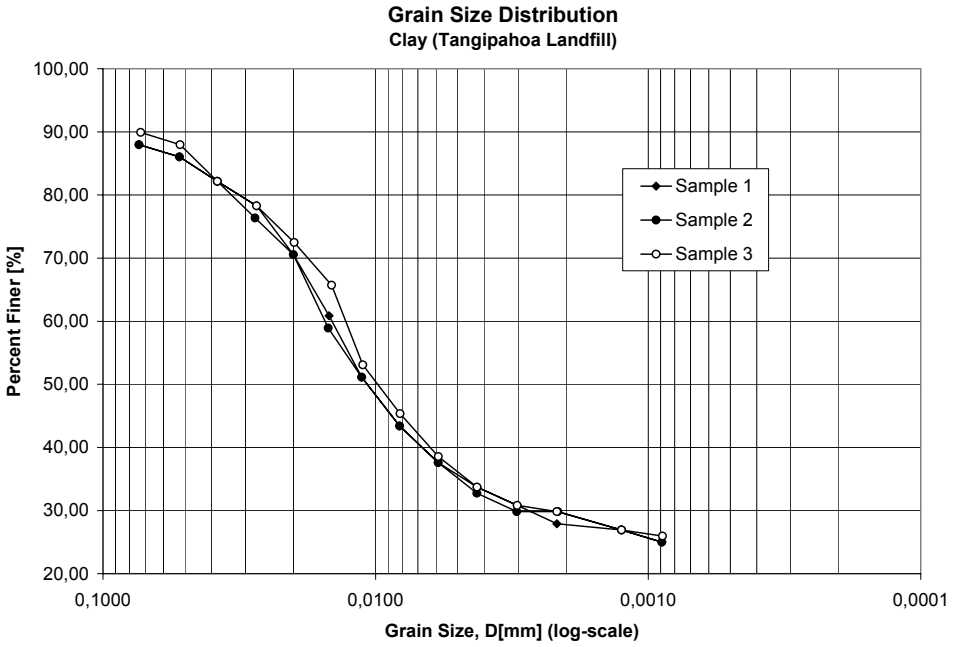

Figure 8. Grain-size distribution of clay used in the first phase of tests (After McManis et al., (2002)).

Commercially available 20/40 sand (crystalline silica) was used for the top and bottom sand layers.

The model piles tested were 1-inch (2.54 cm) in diameter. As control, one chamber was assembled without a pile and one chamber was assembled with an "almost full-length sand pile" to represent the best and worst possible cases for flow. The compaction of the clay was followed by driving the steel and wood piles. Piles used for the tests fully penetrated the clay layer into the lower sand. The round steel pile and the H-section pile have the same cross section along their axis. Both wooden piles, treated and untreated, were tapered according to ASTM D25 (Standard Specifications for Round Timber Piling). The taper starts 5-inch (12.70 cm) from the butt with 1-inch (2.54 cm) diameter and ends at the pile's tip with a diameter of 0.85 inch (2.16 cm).

4.4.1 Installation of piles

The following Pile-Test Chambers were assembled and tested:

Chamber A	No pile
Chamber B	Sand pile (Circular)
Chamber C	Steel pile (Circular)
Chamber D	Treated wood (Circular)
Chamber E	Untreated wood (Circular)
Chamber F	Steel pile (H-Section)

Table 1. Pile types tested in the first phase by Boutwell et al., (2000).

Chamber A served as a control chamber and no pile was installed in it. Chambers C through F had driven piles installed after the clay was compacted. A guide placed on top of the chamber was used to drive the piles vertically. Once the guide was attached, the whole chamber was placed into a hydraulic press. After driving the pile half way, the chamber was removed from the press and the piles were driven slowly. The tip of the pile penetrated 1 inch into the lower sand, below the clay layer. To assure that all piles were driven through the clay layer, measurements from the top were used as a control.

For the sand pile (Chamber B), a steel pile was placed before compaction of the clay, ending 1 inch above the lower sand layer. After the clay was compacted in the chamber, the steel pile was removed and the remaining cavity was filled with sand.

4.5 Tests

To test the different piles, six identical chambers were assembled. They were all supplied with the permeant from one tank, which is pressurized by air from its top. The same air pressure line supplies the chambers' rubber tubes for simulating the overburden pressure. The overburden pressure in each chamber can be regulated separately. The fluid pressure applied was held constant at 15 psi (103 kPa) throughout the whole test. This is equivalent to 34.00 ft (10.54 m) head of water. The permeant first enters the upper sand stratum where it is uniformly distributed due to the high permeability of the sand.

A sketch of the test set-up and the associated supply equipment and manifold is shown in Figure 9. A photograph of an assembled test set up in the laboratory is shown in Figure 10.

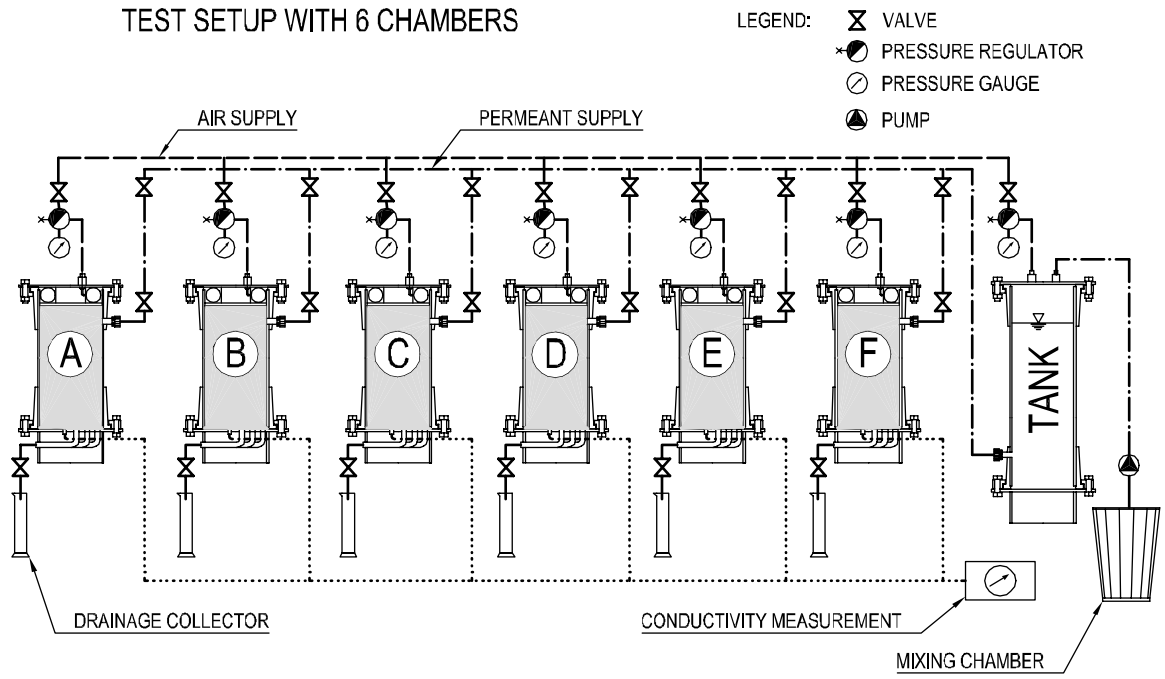

Figure 9. Schematic of test setup with 6 chambers and supply manifold

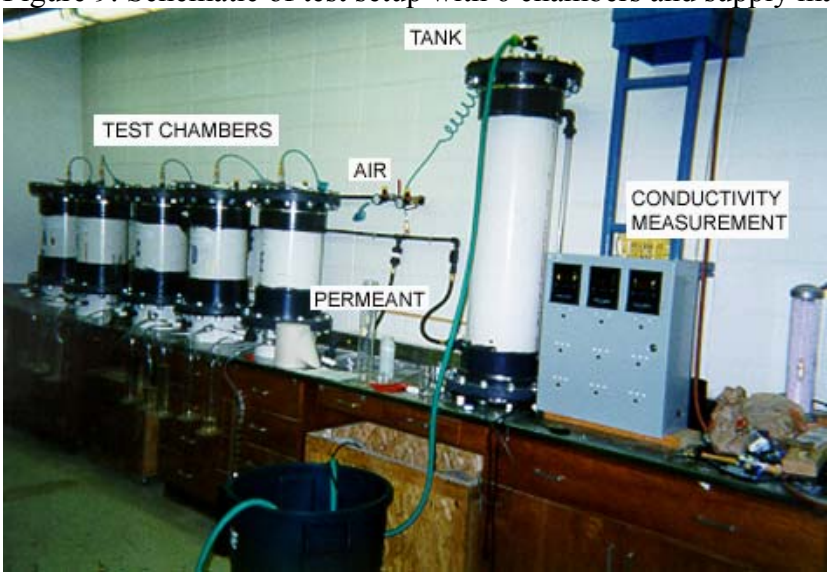

Figure 10. Test Set-up for 6 Chambers (chamber F not installed) and Supply Manifold

4.6 Analysis and Results [First Phase]

4.6.1 Hydraulic Conductivity

During the test, flows from the center, middle and outer regions were recorded seperately. The hydraulic conductivity of each region was computed on the basis of Darcy's Law:

$$v = k \cdot i = k \cdot \frac{\Delta H}{\Delta L} \qquad (1)$$

where

v [cm/s] = average flow velocity in vertical direction

ΔH [m] = difference of fluid pressure heads

ΔL [m] = length of the flow path.

Figure 11 shows a typical plot of variation of hydraulic conductivity with time for chamber C, which had a circular steel pile fully penetrating the clay layer. The permeant for the phase illustrated in Figure 11 was water.

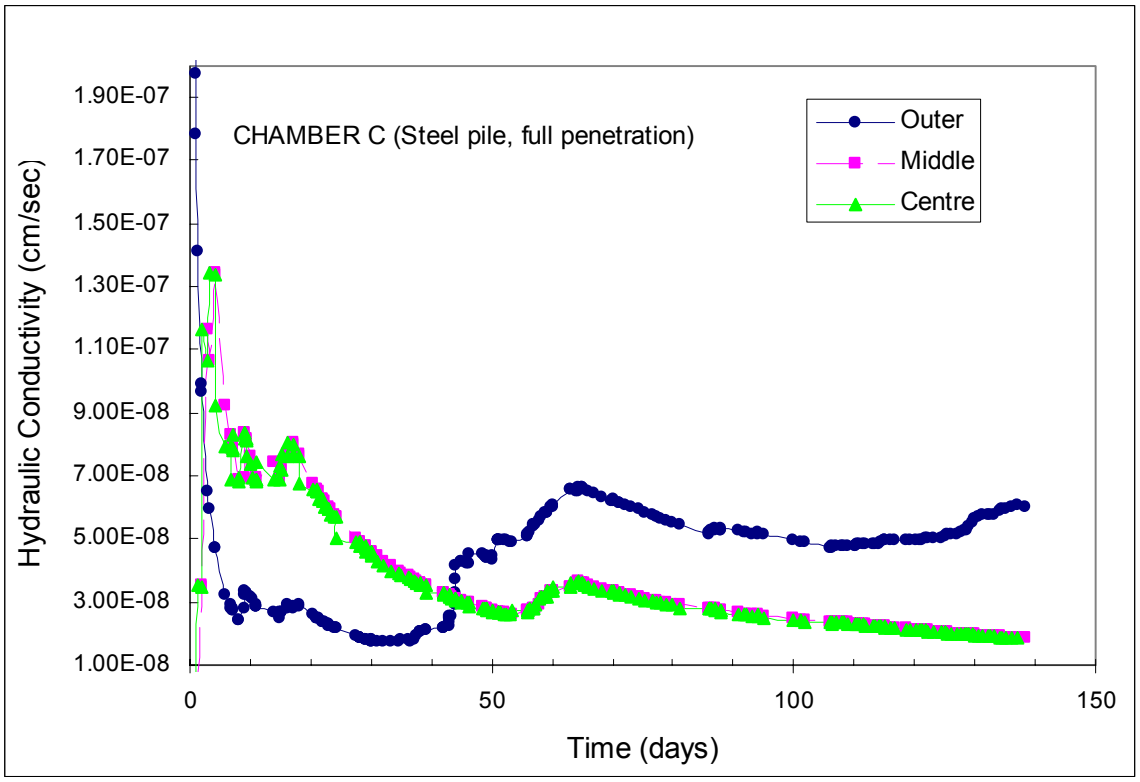

Figure 11.Typical plot of hydraulic conductivity versus time for chamber C, having a circular steel pile fully penetrating the clay layer.

The variation of hydraulic conductivity is apparent in Figure 11. The hydraulic conductivity for this chamber was initially high and later stabilized as seen. The middle and the center areas follow closely where as the outer region shows higher hydraulic conductivity.

As the center region is most affected by the piling, the chambers were compared on the basis of hydraulic conductivity of the center regions. The average hydraulic conductivities from the water phase for all model piles tested in the first phase are plotted in Figure 12.

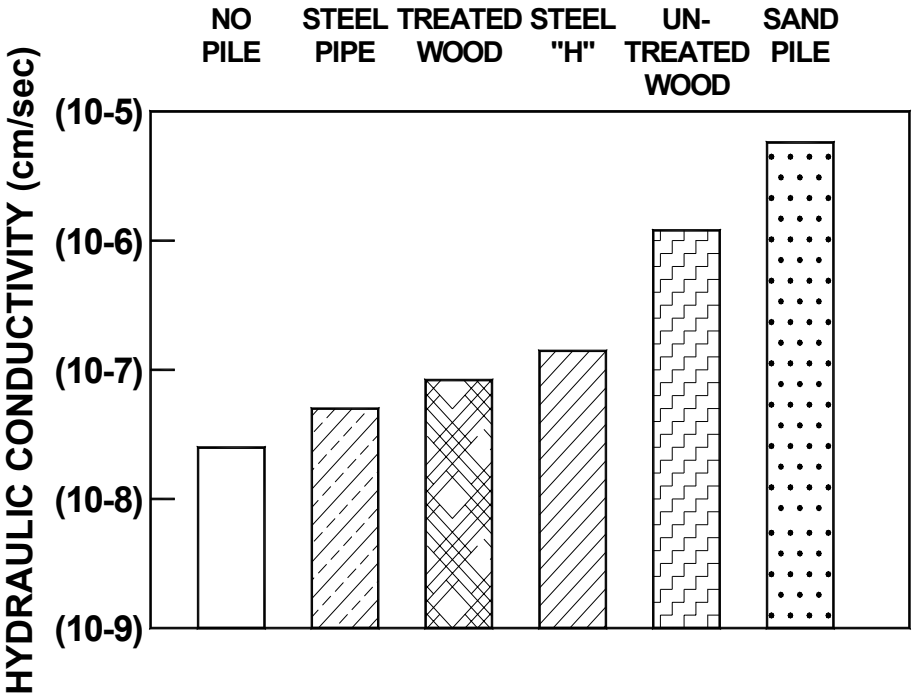

Figure 12. Plot of hydraulic conductivity from the center ring (McManis et al, 2002).

Comparing the hydraulic conductivity results, the different piles are ranked below (in descending order- highest permeability to lowest)

Chamber B	Sand Pile
Chamber D	Untreated Wood
Chamber F	H-Section Pile
Chamber E	Treated Wood Pile
Chamber C	Steel Pile

4.6.2 Electrical Conductivity (Contaminant Transport)

The second phase of the tests used brine as the permeant. Electrical conductivity measurements were taken along with the flow measurements. The correlation between the electrical conductivity measurement and the brine concentration is presented in Appendix I. The contaminant transport was observed to occur in two stages; the first stage included a rapid increase of concentration of brine over time. This may be due to the mixing process of contaminants with the stored un-ionized water and the purging of clear water from the pore volume. Adsorption is assumed to play a minor role during the initial stage when the permeant is water. During the second stage, when Brine is the permeant very less increase in concentration was observed. Chlorine is a conservative tracer and is hardly adsorbed. The results of the contaminant transport for the inner region are presented in Figure 13.

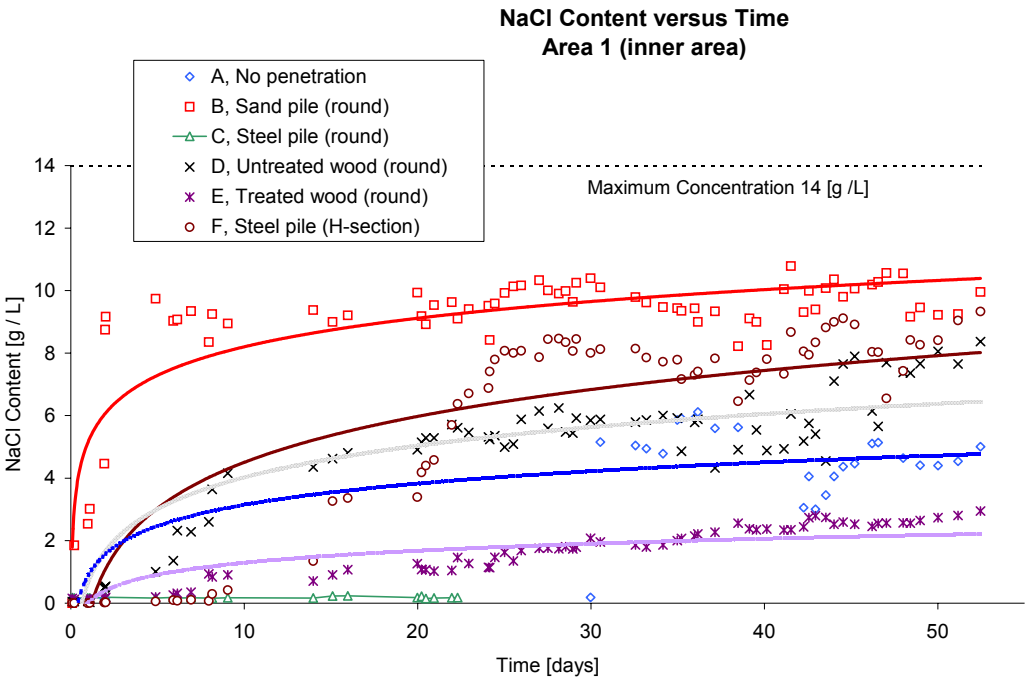

Figure 13. NaCl – content versus time for area 1 (center area)

The electrical conductivity measurements during the brine permeation phase showed the "contaminant" transport behavior of the various test cases. The contaminant transport measurements were simplified using relative concentration (R_c). This is defined as ratio of difference in measured conductivity (c) and background conductivity (c_o) to the difference in input brine conductivity (c_b) and background conductivity (c_o)

$$[R_c = (c-c_o)/(c_b-c_o)]. \qquad (2)$$

Again, only data from the innermost collection ring was analyzed. The results are presented in Figure 14.

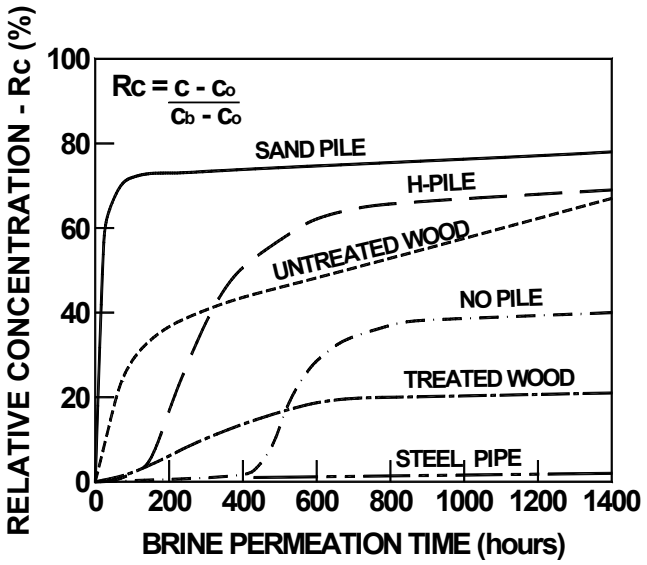

Figure 14. Relative Brine Concentration over Time (McManis et al ., 2002).

The increase in relative concentration for the circular steel pile and the treated wood pile are minimal compared to the other cases.

These piles were driven and pile driving may have densified the soil around the pile. This densification in turn may have reduced the hydraulic conductivity slightly. The effect of pile installation will be discussed in a separate chapter. The untreated wood and steel "H" piles showed increases in relative concentration approaching those for the sand pile case.

4.7 Analytical Study on Direct Transfer

An analytical study was conducted by Boutwell et al., (2000) to model direct transfer phenomena. Consider a single pile with a flat tip driven into the clay layer. As the pile is driven into the clay, a soil plug is formed at the pile tip. This soil plug will be pushed along with the pile. The volume of the soil plug at the pile tip can be approximated as $0.15\ D_p^3$, where D_p is the diameter of the circular pile or width of the square pile. The pore water present in this soil plug will have the same contaminant concentration as that in the upper stratum (c_o). The actual volume of the contaminant in the soil plug is $n\ 0.15\ D_p^3$, where "n" is the porosity of the soil. Frictional drag may reduce the volume of the plug and hence the amount of contaminant present in the plug. The actual volume of the contaminant in the soil plug is proportional to the cube of diameter of the pile tip. Conical pile tips can be used to reduce the volume of contaminant. The use of a conical tip leads to the formation of a smaller soil plug. The smaller soil plug will have a lesser volume and hence will contain less contaminant relative to the flat tip pile. For a steel pile with a circular conical tip, the contaminant transfer is 0.3% of the theoretical maximum for a steel pile with a flat tip. Similarly a wooden pile with a conical tip transfers 7% of the theoretical maximum of a wooden pile with a flat tip.

Hayman, et al., (1993) termed the direct transfer due to pile driving as “dragdown”. For a hypothetical plant process construction area of 2,50,000 square feet with an average pile spacing of 40 feet, the dilution factor was found to be 6.0 parts per billion. This indicates that an original concentration of 1000 mg/L (ppm) would be reduced to less than 0.01 µg/L (ppb). The regulatory concerns have to be addressed by considering the maximum concentration downgradient of a pile group in a flowing aquifer. Figure 15 indicates a reduction in the concentration caused by the soil slug as the plume moves away from the pile.

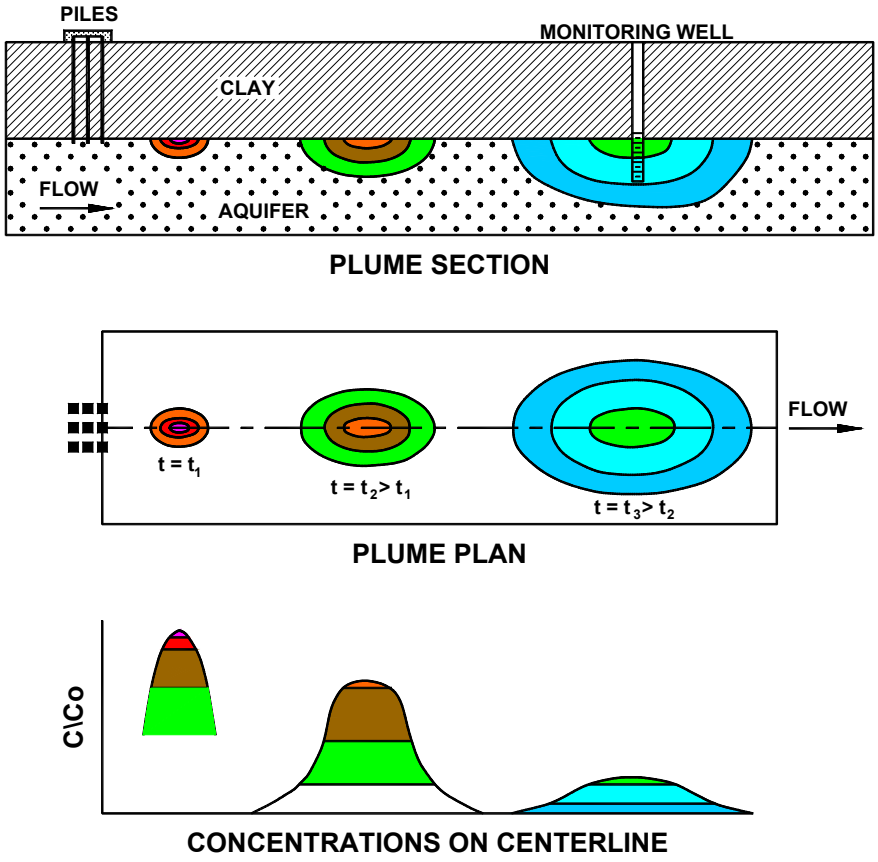

Figure 15. Plume due to direct transfer. (McManis et al., 2002)

Baetsle (1969) developed a three dimensional advection-dispersion model for an instantaneous solute point source in an infinite, homogeneous three dimensional domain with uniform groundwater flow. This model can be used to describe the reduction in concentration with time and distance from the pile. This model has conservative assumptions of the aquifer being homogeneous and isotropic. Also, the contaminant is regarded to be miscible, non-degradable, non-reactive and non-adsorptive to the aquifer.

Diffusion can be neglected, as dispersion dominates at the relatively high groundwater velocities and are the governing terms in Baestle's equation. The analytical solution for the ratio of contaminant concentration in the plume (c/c_o) is given by:

$$\frac{c}{c_0} = \frac{V_e \sqrt{pq}\, e^{-F}}{8(\pi \alpha X)^{3/2}} \qquad (3)$$

where

$$F = \frac{1}{4\alpha X} \cdot \left[(x - X)^2 + py^2 + qz^2 \right]$$

c = Contaminant concentration in plume

c_0 = Initial contaminant concentration

F = Factor accounting for location of the plume

V_e = Effective pore volume of the plug

α_I = Characteristic length, direction (i)

$p = \alpha_x / \alpha_y$

$q = \alpha_x / \alpha_z$

x = Location of (c/c_0) along flow axis (x)

y = Location of (c/c_0) , horizontally from x axis

z = Location of (c/c_0) , vertically from x axis

X = Location of the plume center along the flow axis = v' t

v' = v / n_s , where n_s = porosity of aquifer

v = gross water velocity = k i

i = Hydraulic gradient in the aquifer

k = Hydraulic conductivity of the aquifer material

The contaminant plume has been considered to be fairly uniform in concentration near its centre for large relative distances ($\alpha X > 20$). The Baetsle equation can then be approximated by:

$$\frac{c_m}{c_0} = \frac{NV_e\sqrt{pq}}{8(\pi\alpha X')^{3/2}} \qquad (4)$$

Here, c_m represents the maximum concentration in the plume at the distance X' from the pile. The number of piles in the pile group is denoted by N, and X' represents the distance from the pile group center.

The end bearing resistance of a pile driven into a cohesionless soil (aquifer) usually forms a major component of the pile resistance. As the overlying clay prevents upward flow, all the flow is in the aquifer. Doubling the contaminant volume will account for this.

The principle of superposition can be used to analyze multiple pile groups using Equation 3. For large relative distances ($\alpha X > 20$) Equation 4 is to be used.

The maximum ratio of contaminant concentration in the plume versus the initial contaminant concentration is denoted by (c_m/c_0). Figure 16 is a plot of (c_m/c_0) versus various distances from the downgradient pile faces, for a single pile and for a group of 9 piles.

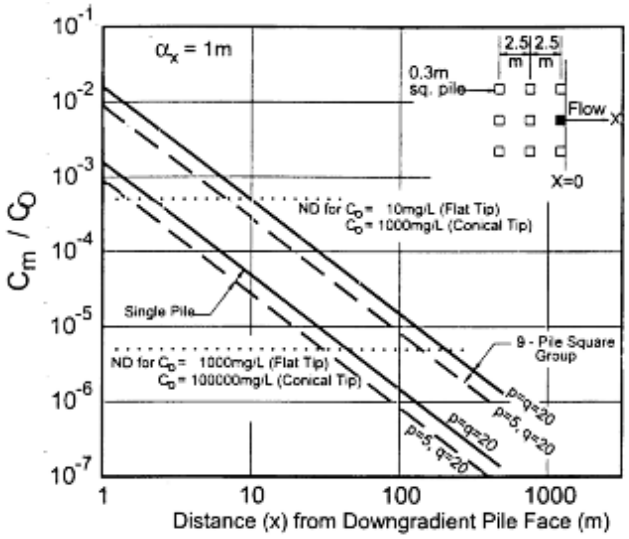

Figure 16 – Dilution of Direct Transfer Contaminants (Boutwell et al., 2000)

The U.S. EPA specifies the Maximum Contaminant Level (MCL): The highest level of a contaminant that EPA allows in groundwater. Figure 16 allows the measurement of the distance (x_c) from the pile group at which the concentrations of various common types of contaminants reaches the MCL.

Some of the common industrial contaminants include petroleum hydrocarbons, heavy metals, and/or volatile organics. Assuming the "worst case" scenario of flat tipped piles, the distance x_o can be calculated for various concentrations of the industrial contaminants. The results for common industrial contaminants are presented in Table 2.

Group	MCL (mg/L)	Single Pile x_c (feet)		9 - Pile Group x_c (feet)	
		c_o = 10 mg/L	c_o = 1000 mg/L	c_o = 10 mg/L	c_o = 1000 mg/L
Pet. Hydrocarbon	0.34	<3	10	<3	30
Heavy Metals	0.015	3	60	12	240
Volatile Organics	0.005	6	140	25	550

Table 2. Distances Downgradient to C_m<MCL (Boutwell et al., 2000).

The results presented in Table 2 indicate negligible amounts of contaminant transport by direct transfer for the assumed "worst case" (flat tip piles).

The use of a conical tip significantly reduces the volume of contaminant by 1 to almost 3 orders of magnitude (Hayman et al., 1993). From Meyerhof., (1961) it can be shown that a pile with a conical tip can obtain the same capacity of a flat tip pile if penetration of the tip into the sand is increased by 0.5 to 1.0 times the pile width. For typical cases this represents 1% to 2% additional pile length, which is considerably economical compared to surface casing, and will satisfy the regulatory requirements.

Boutwell et al., (2000) suggest that the use of a 45^o conical tips in a 9-pile group reduces the distance (x_c) at which $c_m < 0.005$ mg/L for $c_o = 1000$ mg/L from over 450 feet (137 m) to less than 30 ft (9 m).

4.8 Conclusions [First Phase]

The conclusions (McManis et al., 2002) from this phase of investigation are:

- Displacement-type piles (wood, steel, and probably concrete) do not form conduits for contaminant migration.

- Non-displacement piles (steel "H") do form such conduits.

- Untreated wood allows contaminant "wicking", but treated wood does not.

- The effect of Direct Transfer (plug) is negligible, and can be made virtually undetectable by using pointed pile tips.

This investigation suggests that piles can be safely used in brownfields by suitable selection of the pile material and use of a pointed tip.

5. MODEL TESTS (SECOND PHASE)

The first phase of the study was extended to study the behavior of concrete piles. Concrete piles are widely used in practice. The various methods of installation and shapes of concrete piles make them suitable for a wide range of applications. Thus the research of contaminant transport through concrete piles had to focus on the shape of the pile and the method of installation.

5.1 Methodology of Investigation

The investigation included both model tests and numerical studies. The model tests were done using the same test set up described earlier. Numerical studies were conducted to determine the effect of pile penetration on contaminant transport and the effect of pile groups on contaminant transport. The numerical modeling and the results will be discussed in Chapter 5.

As with most prototype testing, a few modifications were made to the prior test set up. The modifications are:

- A clear standpipe of 0.50 in (1.27 cm) diameter and height of about 8.00 in (20.32 cm) was fixed to the flow outlets. This was done to prevent drainage of the permeant from the lower sand layer. The clear pipe enabled detection of any clogs or entrapped air in the system.
- To prevent sand intrusion and subsequent puncture of the rubber tube, a geotextile layer was used to encase the rubber tube.
- In order to minimize wall effects, grooves were made in the clay along the periphery of the wall of the chamber.

The grooves were 1 in (2.54 cm) deep and 1 in (2.54 cm) wide and were cut at an angle of 45^{o} from the chamber wall using a laboratory knife. For each layer, powdered bentonite was placed in the grooves. Bentonite was put along the walls of the chambers at every 3-4 in (7-10 cm) layer except the layer immediately below the top sand layer.

5.2 Properties of Soils Used.

The compacted clay layer simulates the aquitard. For the second series with concrete piles, the clay was obtained from the Tangipahoa Parish Regional Solid Waste Facility. The grain size distribution curve for this clay is shown in Figure 17. The classification properties of this clay were determined using standard ASTM methods. The liquid limit of the clay is 26 with a plastic limit of 14, and the clay is classified as CL as per the Unified Soil Classification System (ASTM D 2487). The standard Proctor compaction test was carried out to determine the compaction properties of this soil, as per ASTM D 698. The maximum dry density was 17.6 kN/m^3 (112 lb/cu.ft) and optimum moisture content was 14.5 %. The soil used had 55% fines (clay and silt) and 45% sand.

Commercially available clean sand (crystalline silica) having a maximum dry density of 101.77 lb/ft^3 (16 kN/m^3) was used for the sand layers at the top and bottom of the chamber.

A comparison between the properties of the clay used in the first phase and the second phase tests is presented in Table 3.

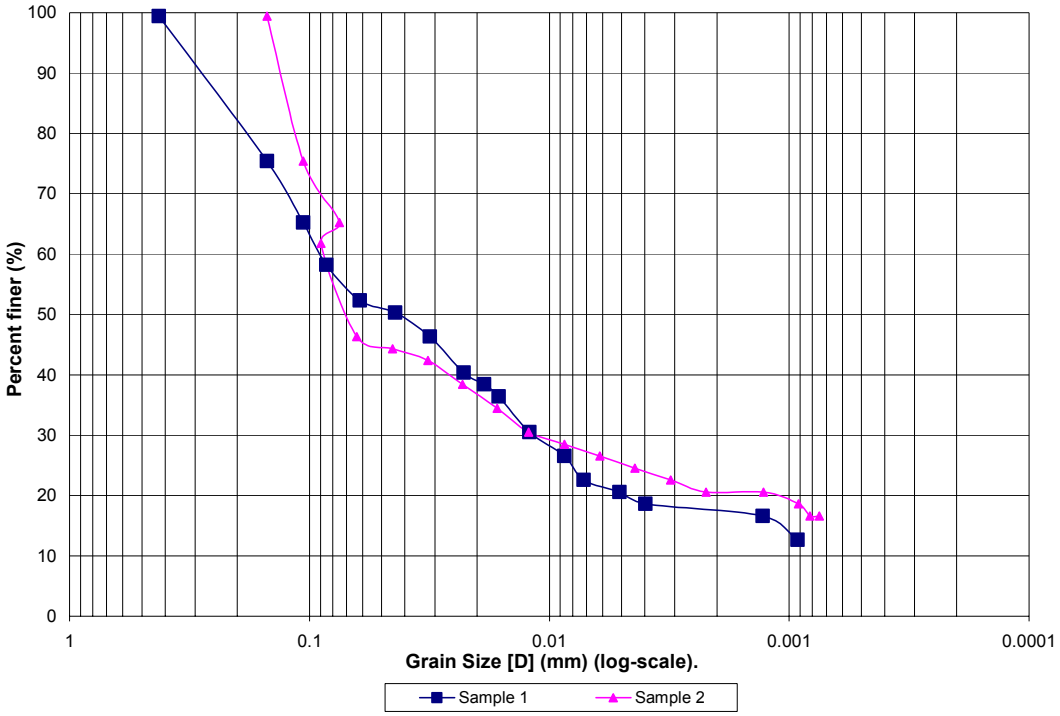

Figure 17. Grain size distribution of clay used in the second phase.

Clay Properties	**Boutwell et al .,(2000); McManis et al., (2002)**	**Present Investigation**
Liquid Limit	34	26
Plastic Limit	15	14
Plasticity Index	19	12
Max. Dry Density (kN/m^3)	18.20	17.60
O.M.C (%)	14.50	14.50

Table 3. Comparison of properties of clay used for model tests at UNO.

5.3 Model Piles

In this study, the effects of 1) depth of penetration, 2) shape of pile and 3) method of installation on potential contaminant transport were investigated. To determine the effect of depth of penetration, the depth of pile embedment into the clay layer was varied. With reference to Figure 18, "L_c" denotes the height of the clay layer; "L_p" represents the depth of pile embedment. "Relative Penetration" is the ratio L_p/L_c and can be used to denote the embedment lengths. The values of ratio L_p/L_c considered for the tests are 0.80 and 1.00. The numerical study involved relative penetrations of 0.5, 0.8, 0.88, 0.92, 0.96 and 1.00. Preliminary numerical studies showed no influence of (L_p/L_c) less than 0.5 on groundwater flow. Thus, model tests included only penetrations of 0.80 and 1.00.

It is to be noted that $L_p/L_c = 1$, signifies full embedment of the pile. In other words, the pile penetrates the clay layer completely as shown in Figure 18(a). The partial embedment cases for $L_p/L_c = 0.8$ and 0.5 are shown in Figure 18 (b) and 18 (c).

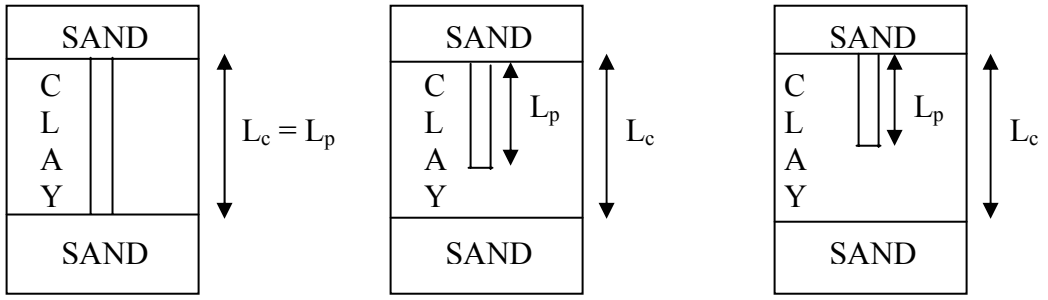

(a) $L_p/L_c = 1$ (b) $L_p/L_c = 0.8$ (c) $L_p/L_c = 0.5$

Figure 18-Schematic representation of various depths of pile embedment.

Table 4 provides a summary of the model pile tests conducted by Haymann et al., 1993, McManis et al., 2002 and the present study.

TESTED BY	D_p (cm)	L_p/L_c	TIP	MATERIAL	SHAPE	INSTALLATION	PERMEANT	MEASURED	
								TIP	FLOW
Hayman et al .,(1993)	1.27	1.17	CONE	STEEL	CIRCULAR	DRIVEN	PCE + TCE	Y	Y
SILTY CLAY LL = 42	1.27	1.17	CONE	WOOD, UNTREATED	DOWEL	DRIVEN	PCE + TCE	Y	Y
									Y
Boutwell et al.,(2000)	-	-	-	(A) NO PILE	-	-	WATER, BRINE	N	Y
and McManis et al.,	2.54	1.67	FLAT	(C) STEEL	CIRCULAR	DRIVEN	WATER, BRINE	N	Y
(2002)	2.54	1.67	FLAT	(F) STEEL	H-SHAPE	DRIVEN	WATER, BRINE	N	Y
SANDY CLAY	2.54	1.67	FLAT	(E) WOOD, UNTREATED	CIRCULAR	DRIVEN	WATER, BRINE	N	Y
LL = 34	2.54	1.67	FLAT	(D) WOOD, TREATED	CIRCULAR	DRIVEN	WATER, BRINE	N	Y
	2.54	1.67	FLAT	(B) SAND	CIRCULAR	CAST-IN-PLACE	WATER, BRINE	N	Y
Present Investigation	-	-	-	(A) NO PILE	-	-	WATER, BRINE	N	Y
and Nataraj et al., (2004)	2.54	1.00	FLAT	(B) CONCRETE	CIRCULAR	DRIVEN	WATER, BRINE	N	Y
	2.54	1.00	FLAT	(C) CONCRETE	CIRCULAR	CAST-IN-PLACE	WATER, BRINE	N	Y
	2.54	0.80	FLAT	(E) CONCRETE	CIRCULAR	CAST-IN-PLACE	WATER, BRINE	N	Y
	2.54	1.00	FLAT	(D) CONCRETE	SQUARE	DRIVEN	WATER, BRINE	N	Y
	2.54	0.80	FLAT	(F) CONCRETE	SQUARE	DRIVEN	WATER, BRINE	N	Y

PCE = Tetra chlorethylene , TCE = Trichloroethylene.

Table 4. Summary of tests conducted at by Hayman et al., (1993) and at UNO [Boutwell et al., 2000; McManis et al., 2002 and Nataraj et al., (2004) (present study)]

The concrete piles of different lengths were cast in moulds fabricated in the laboratory. The model piles were reinforced with a wire cage. The square piles were cast in a wooden mould; the circular piles were cast using a split-PVC pipe. Standard Portland cement and pea gravel were used for the concrete mix. An admixture was used to facilitate rapid curing and to provide high initial strength. Figure 19 shows the moulds employed to cast the square piles and the reinforcement cage used is also visible. Figure 20 shows the moulds used to cast the circular piles, the reinforcement cage, and a pile that is ready. The piles were cured in water for a minimum of 28 days before being used.

Figure 19. Moulds and reinforcement cage used for casting model square piles.
[After Nataraj et al., 2004]

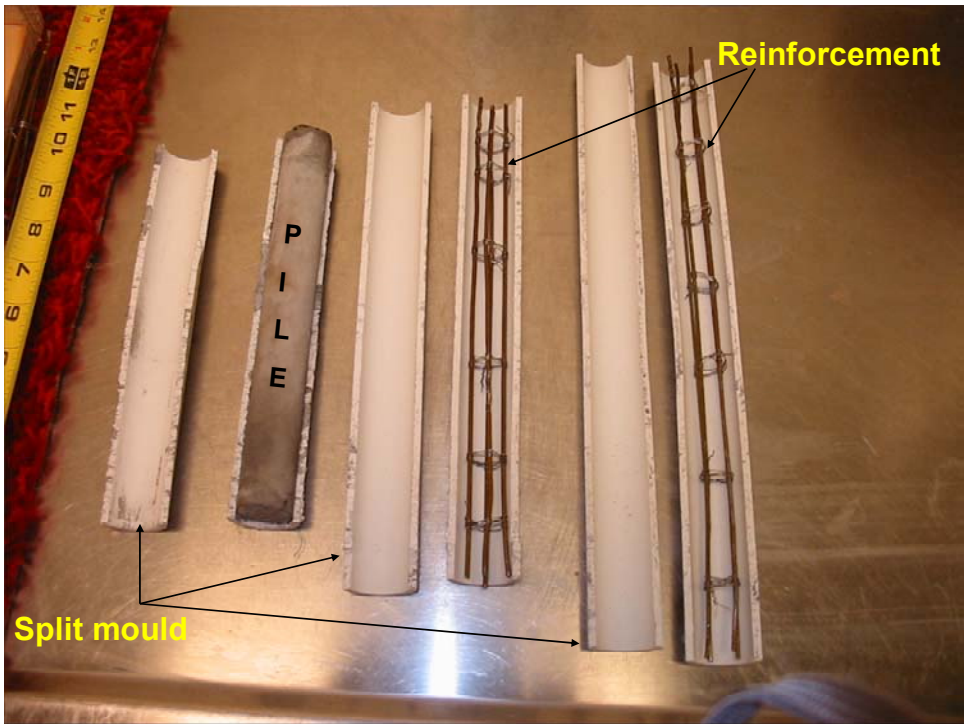

Figure 20. Split moulds used to cast the circular piles. [After Nataraj et al., 2004]

5.4 Test Procedure

The chambers were assembled and the bottom sand layer was poured in place and levelled. Clay was compacted on top of the sand layer in five lifts of equal height using a modified Proctor compaction hammer. The clay was compacted at 95 % of the maximum dry density obtained from the Standard Proctor test on the dry side of the optimum moisture content. After the placement of the first clay lift, a groove with a depth and width of about 1 in (2.54 cm) was cut along the periphery of the chamber. This groove was filled with bentonite clay (in a dry powder form), to provide a seal against flow along the soil wall interface. The successive layers of clay were placed after scarifying the surface of the previous clay layer. After the final layer of clay was placed, sand was filled up to the top of the chamber and lightly compacted leaving sufficient space to accommodate the rubber tube.

To facilitate pile installation and boring of the hole for the cast-in-place piles, a PVC pipe with a diameter of 1.5 in (3.8 cm) and 7.5 in (19.0 cm) high was placed axially centered in the top sand layer. The chamber was then sealed by fastening the top plate. The chamber was then connected to the air supply system and the water tank to initiate the tests. The tests were conducted initially with water as the permeant. The chambers were permeated with water for about 2400 hours before the piles were placed. After placing the piles, brine was used later as the permeant to simulate the contaminant and the tests were continued.

5.5 Installation of the model piles

The model piles involved different methods of installation. Table 4 provides a summary of the different piles used. The precast piles were slowly driven into separate chambers. A guide was used to ensure axial penetration. The piles were slowly driven into the chamber, ensuring that no lateral load was acting on the pile. A circular precast concrete pile completely penetrating the clay layer was driven in chamber B. A square precast pile completely penetrating the clay layer was driven into chamber D, and a square precast pile having a relative penetration (L_p/L_c) of 0.80 was driven into chamber F.

The cast-in-place piles were cast in situ in chambers C and E. Chamber C had a circular cast-in-place pile fully penetrating the clay layer. Chamber E had a circular cast-in-place pile having a relative penetration of 0.80.A circular borehole of the required diameter was made using a commercially available drill. The depth of the borehole was made equal to the depth of penetration desired, 1 ft (30.5 cm) for chamber C ($L_p/L_c = 1$) and 9.6 in (24.4 cm) for chamber E ($L_p/L_c = 0.8$).

A concrete mix was poured into the borehole in layers and each layer was well tamped using a tamping rod. Figure 21 illustrates a typical installation procedure for the model piles.

Boring using a drill to cast the cast in situ pile (left); pile after it was cast (right).

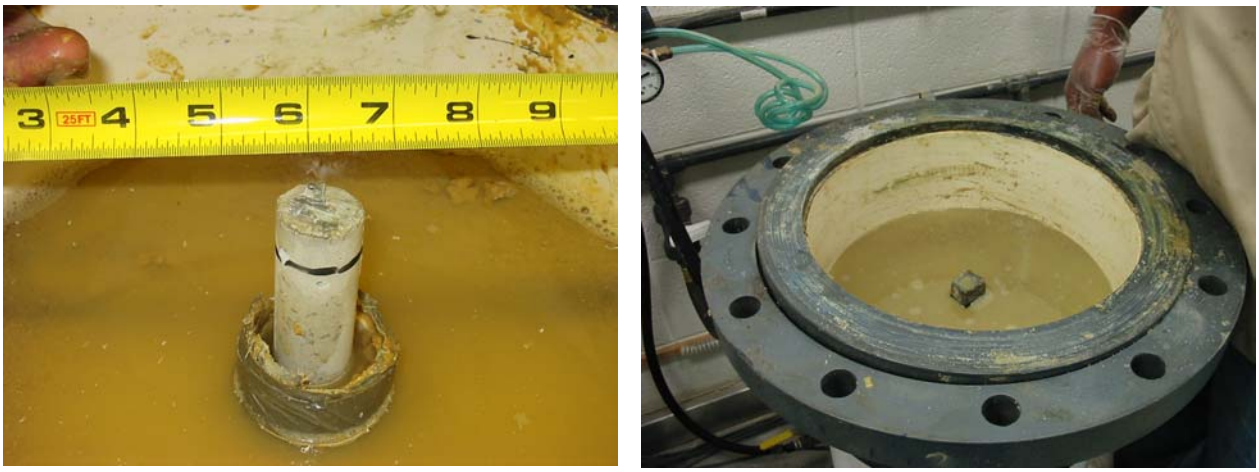

Driving a precast circular pile, the plastic pipe segment installed to facilitate driving is visible (left); the photograph on the right is of a square precast pile after it has been driven.

Figure 21. Various photographs showing pile installation.
[After Nataraj., et al (2004)]

6. TEST CONDITIONS AND DATA ANALYSIS

The one-dimensional Green-Ampt method (Green W.A and Ampt G.A., 1911) was used to estimate the number of days required for saturation of the test chambers. A brief description of this method is given in Appendix II. For an assumed value of hydraulic conductivity equal to 1 X 10^{-8} cm/sec and an air porosity of 0.09, the model predicted 44 days for saturation. The chambers took slightly more time to saturate than predicted, varying from 55-75 days for different chambers. The chambers were initially saturated from the bottom and the flow was then reversed.

For the tests, the overburden pressure was maintained at 14 psi (96 kPa) throughout the tests. The pressure in the water tank (permeant) was kept at 12 psi (82 kPa) throughout the tests. Flow from the chambers was recorded at regular intervals. Periodic measurement of electrical conductivity and flow were recorded. The tests were conducted without any piles and with water as permeant in the first stage for a period of about 2400 hours.

The flow data and the electrical conductivity data were analyzed to determine the effect of pile on flow and contaminant transport.

6.1 Hydraulic Conductivity.

The hydraulic conductivity was computed on the basis of Darcy's Law as in the previous investigation (Boutwell et al., 2000; McManis et al., 2002); see section 4.6.1. The fluid pressure applied was held constant at 14 psi (96 kPa) throughout the whole test. This is equivalent to 32 feet (9.82m) head of water. The change in density due to the salt content is small and can be neglected.

The permeant first enters the upper sand stratum where it is uniformly distributed due to the high permeability of the sand. It then flows through the clay layer and exits through the flow outlets, where it is collected and measured frequently.

Considering only the vertical flow, L_c is the difference in elevation between the upper and lower boundary of the clay layer. Hence L_c = 12 inch (30.5 cm). Hydraulic resistance of the sand layers (above and underneath the clay) is not taken into account for calculating (k). It can be shown that their hydraulic resistance is small compared to the hydraulic resistance of the clay and can be neglected. Hydraulic conductivity (k) was computed using the volume of flow (ΣQ_i) that occurred over a period of time(Δt). The formula employed to compute k_i is given below,

$$k_i = \frac{(\Sigma Q_i)(L_c)}{(\Delta t)(p + L - h)(A_i)} \text{.....} cm/\sec. \qquad (5)$$

where,

subscript "i" denotes the regions and is 1 for center, 2 for middle and 3 for outer.

k_i = hydraulic conductivity of i^{th} region….(cm/sec)

ΣQ_i = volume of flow observed for i^{th} region during time Δt…… (ml)

Δt = time interval during which volume of flow ΣQ was observed……(sec)

p = pressure head of water entering the chamber……(cm)

L_c = height of the clay layer in the chamber = 30.5 cm. (12 in)

h = head measured at the discharge end of the chamber…..(cm).

A_i = area of region through which flow occurred. The areas of center, middle and outer regions are Center A_1 = 81.03 cm^2 (12.56 in^2), Middle A_2 = 243.1 cm^2 (37.68 in^2) and Outer A_3 = 405.2 cm^2 (62.80 in^2).

During testing the following data was recorded:

t [sec] = cumulative time since the start of the test and

Q_i [mL] = cumulative volume drained in an Area i.

An example of computation details of hydraulic conductivity (k) for analysis and plotting purposes is provided in Appendix III. The cumulative volumes of flows observed in the chambers are plotted in Figures 22 and 23. A detailed flow comparison is presented in the inset in these charts.

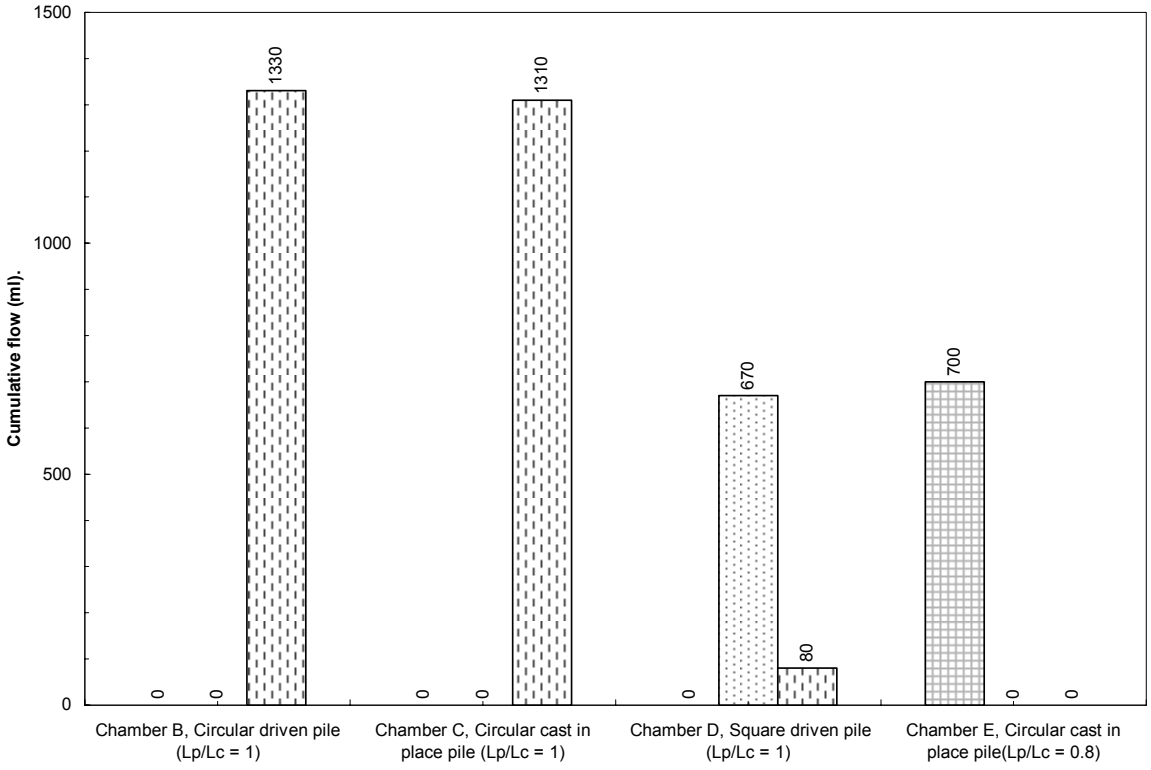

Figure 22. Cumulative volume drained with respect to different areas (Without pile- permeant water)

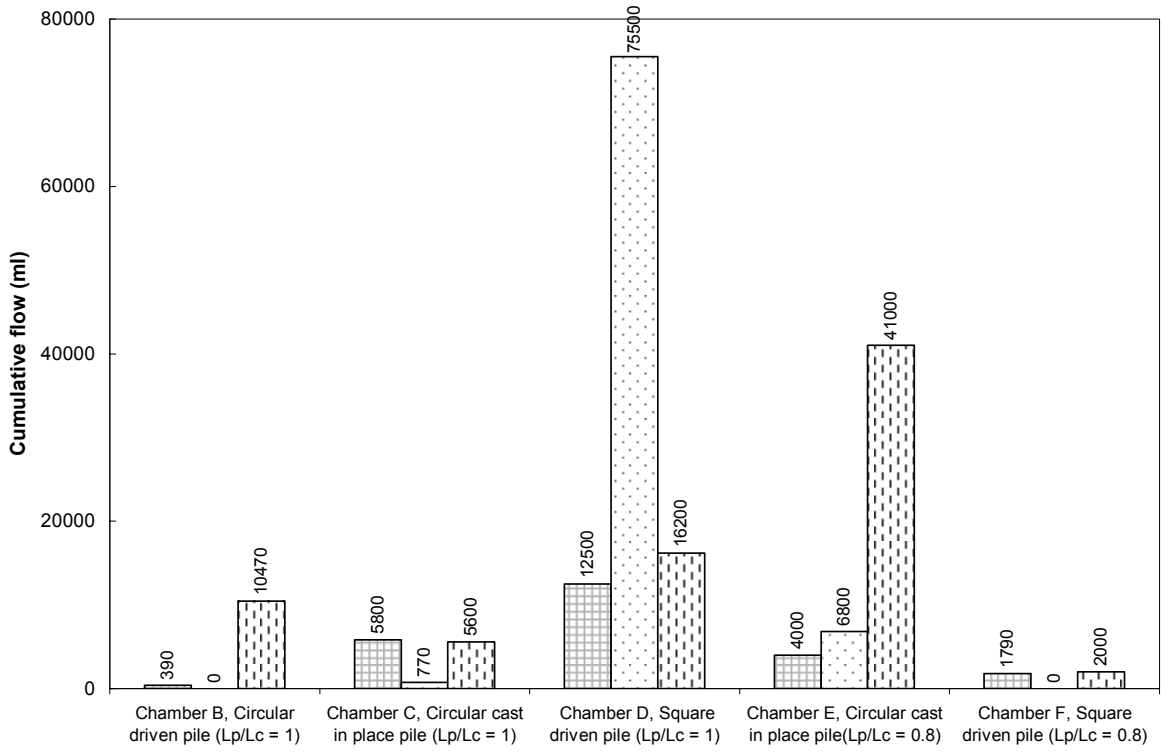

Figure 23. Cumulative volume drained with respect to different areas (With pile- permeant water)

Hydraulic conductivity was computed for all the chambers as described in Appendix III. The various plots of hydraulic conductivity versus cumulative time are given as Figures 24 to 29. The ordinate in Figures 24-29 is the hydraulic conductivity and the abscissa is the cumulative time in days since the start of the test. The initial tests were carried out with water as permeant and without any pile. During this period the chambers saturated and flow was observed from some of the outlets. This is shown by the "Permeant Water No Pile" label on the abscissa in Figure 24.

The pile was introduced after the chamber was saturated. The time of introduction of the pile is different for each individual chamber due to the different saturation periods.

The chambers were permeated with water with piles in place for around 90 days. Brine was then introduced as the permeant and the last reading was recorded on April 31, 2005.

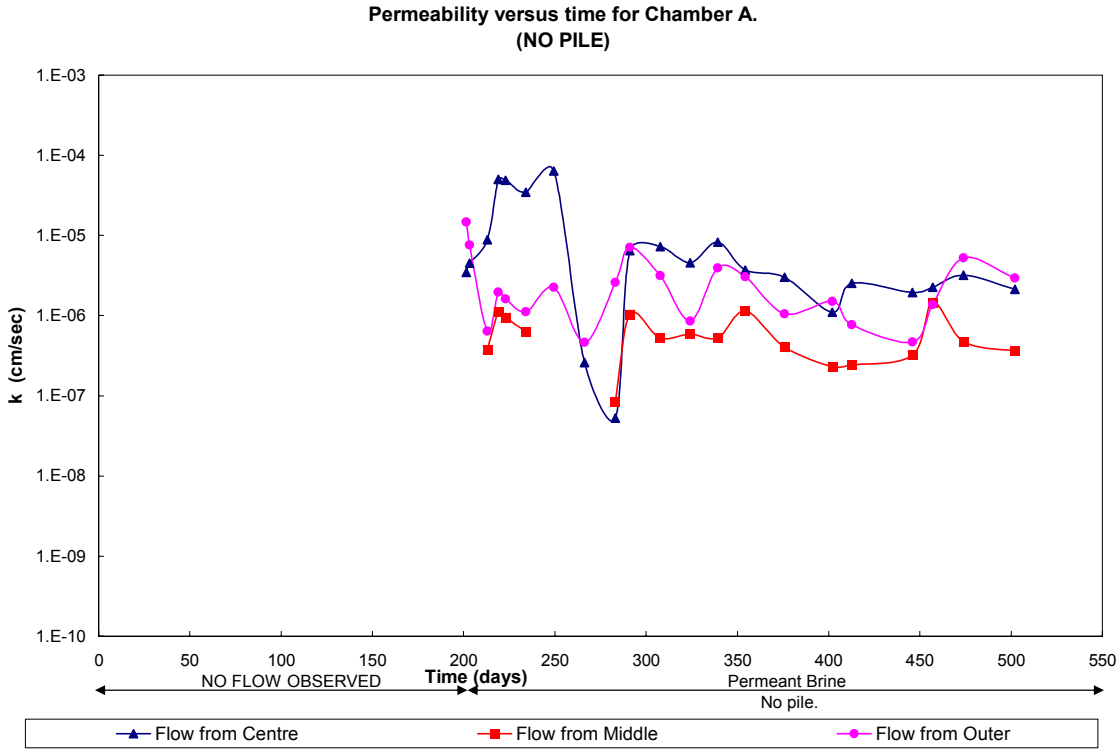

Figure 24. - Hydraulic conductivity versus time for chamber A.

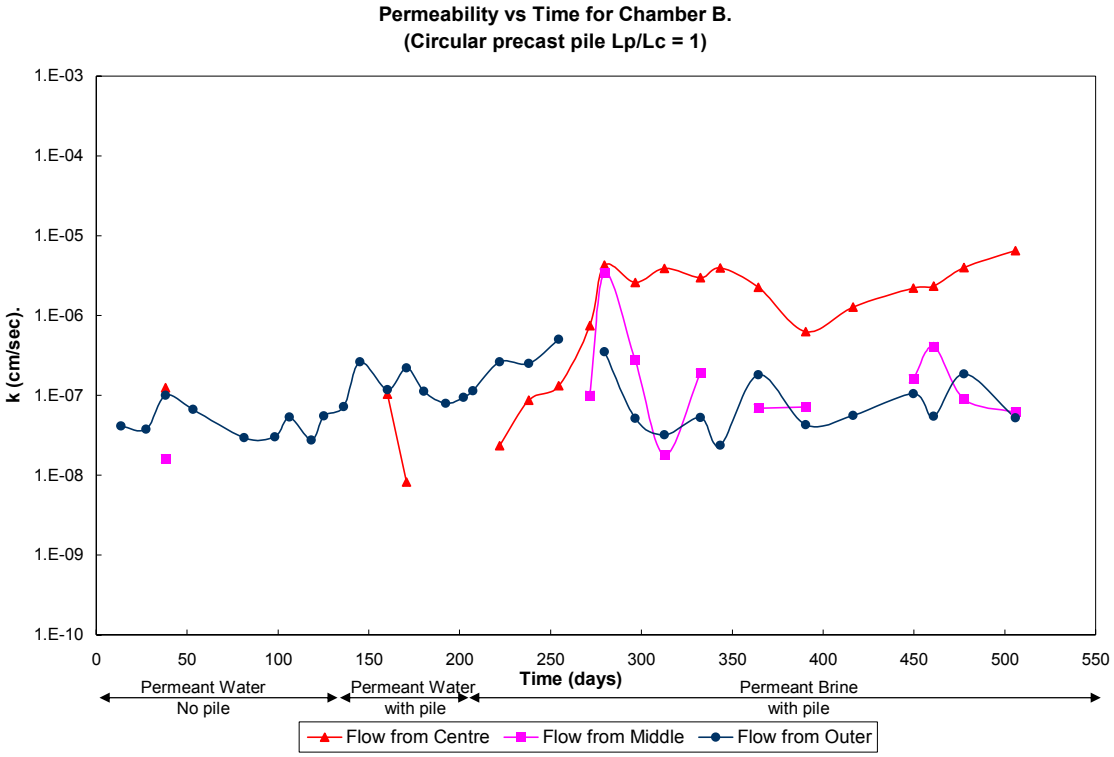

Figure 25.- Hydraulic conductivity versus time for chamber B.

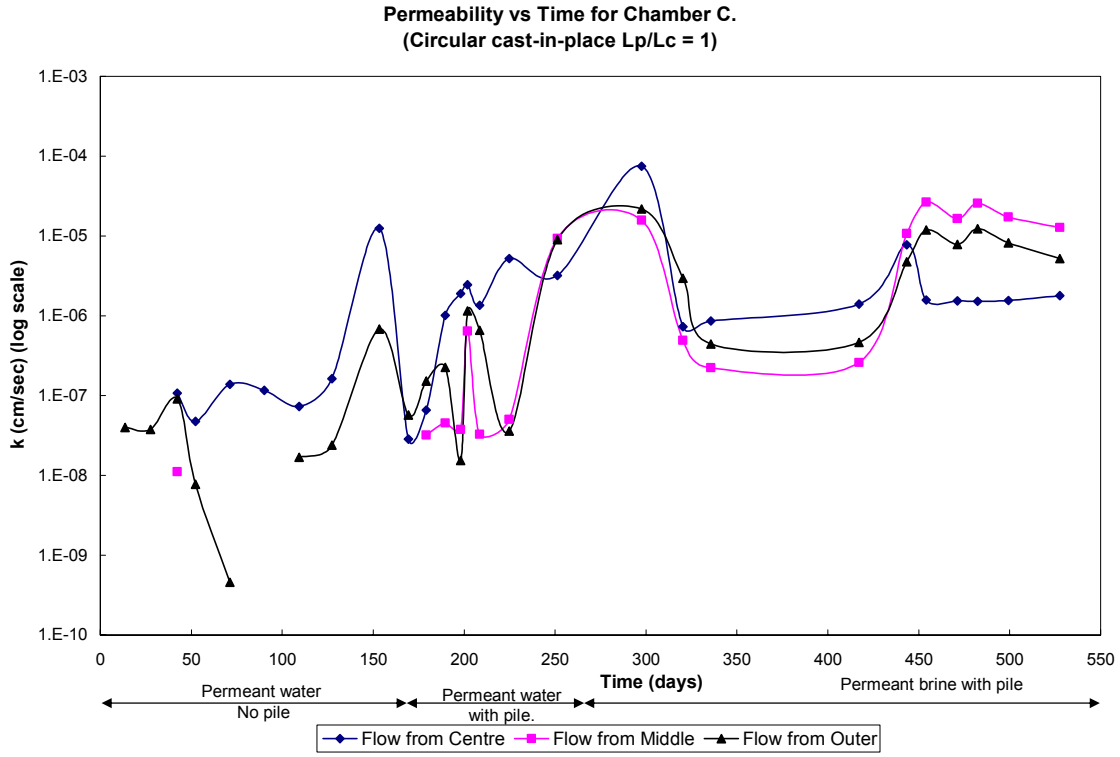

Figure 26.- Hydraulic conductivity versus time for chamber C.

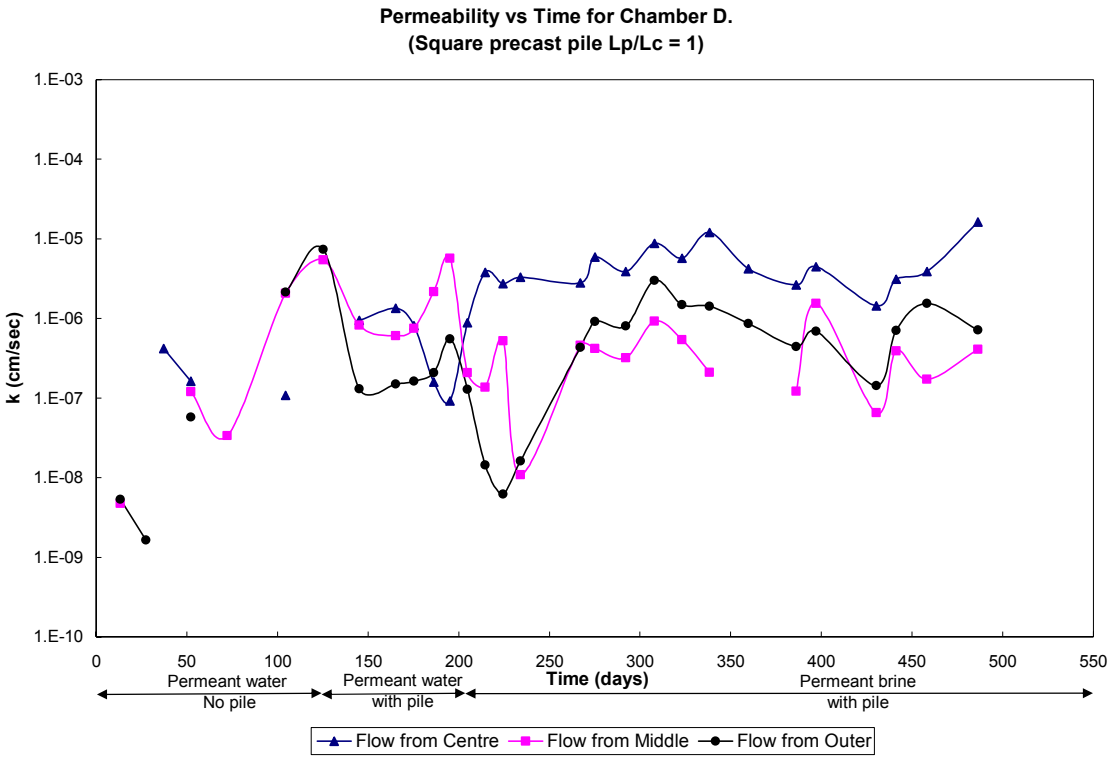

Figure 27.-Hydraulic conductivity versus time for chamber D.

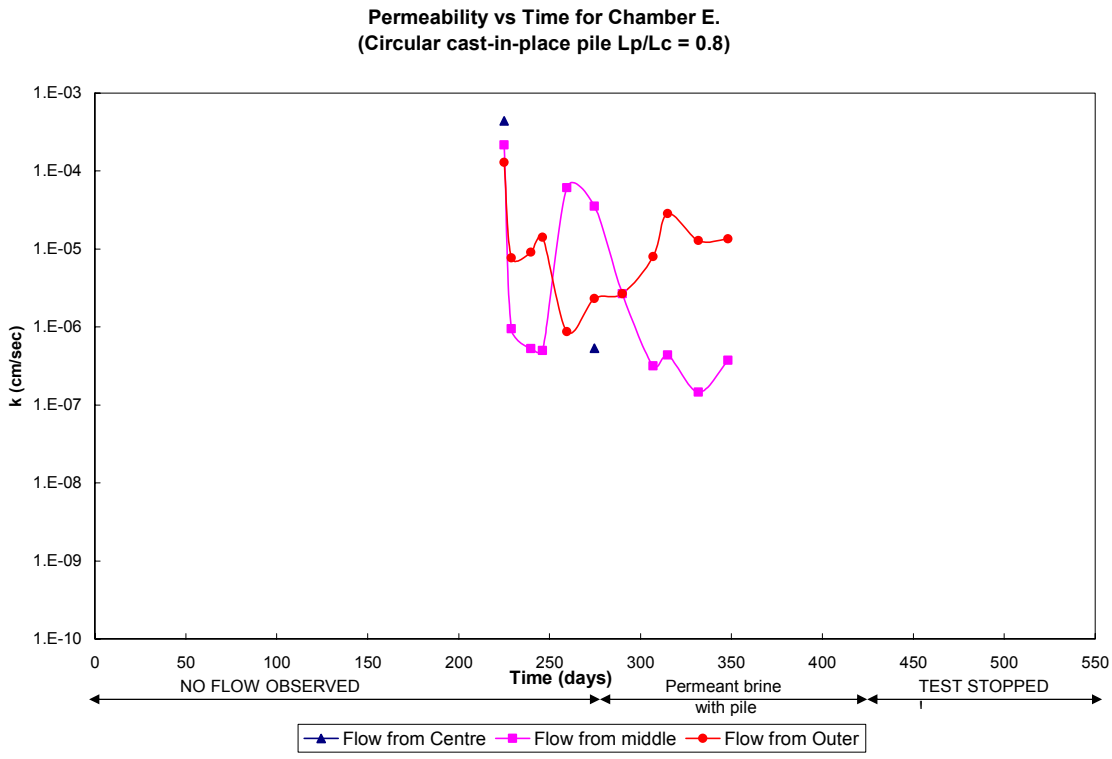

Figure 28. - Hydraulic conductivity versus time for chamber E.

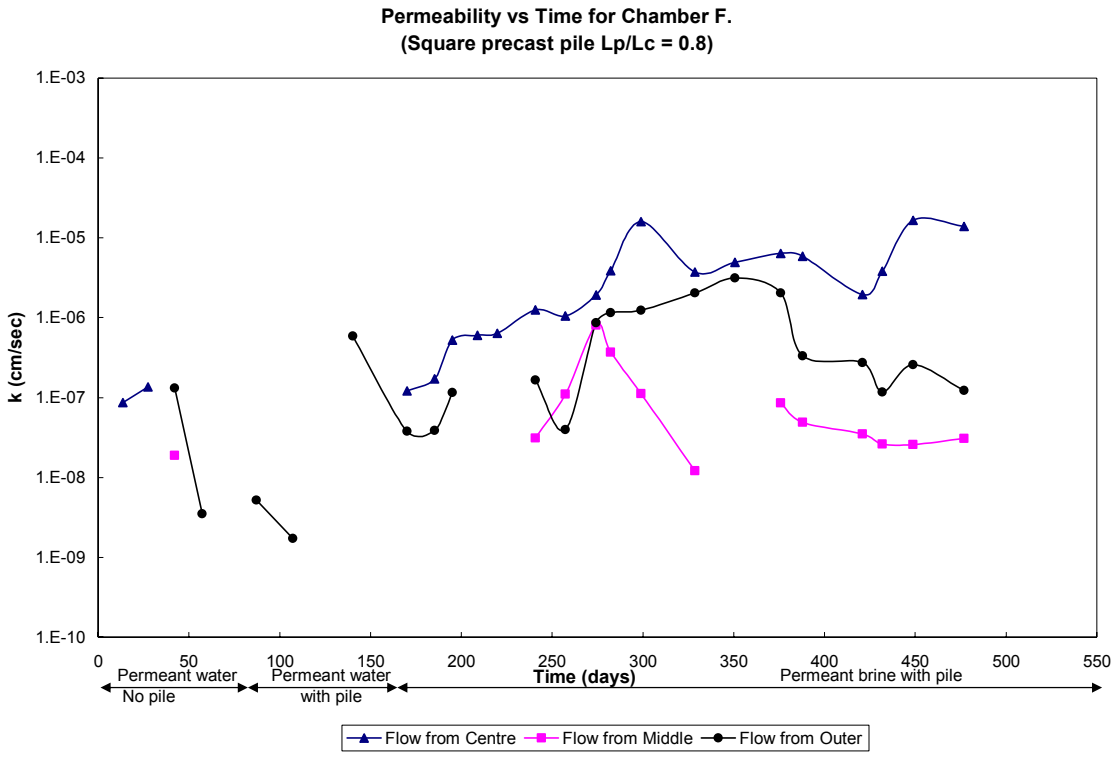

Figure 29. - Hydraulic conductivity versus time for chamber F.

The introduction of the pile increased the hydraulic conductivity somewhat in all the chambers. This may be due to a disturbed zone formed below the pile or the formation of preferential pathways for flow. The hydraulic conductivity increases further with the introduction of brine as permeant.

To determine the increase in hydraulic conductivity caused due the installation of piles, a term "relative flow" was defined. Relative flow is the ratio of the flow from the chambers with pile (Q_p) to the no pile chamber (Q_{np}). This allows the determination of the increment in flow due to pile. The flow results from the first phase of tests (McManis et al., 2002) and those from the present study are compared in Figure 30.

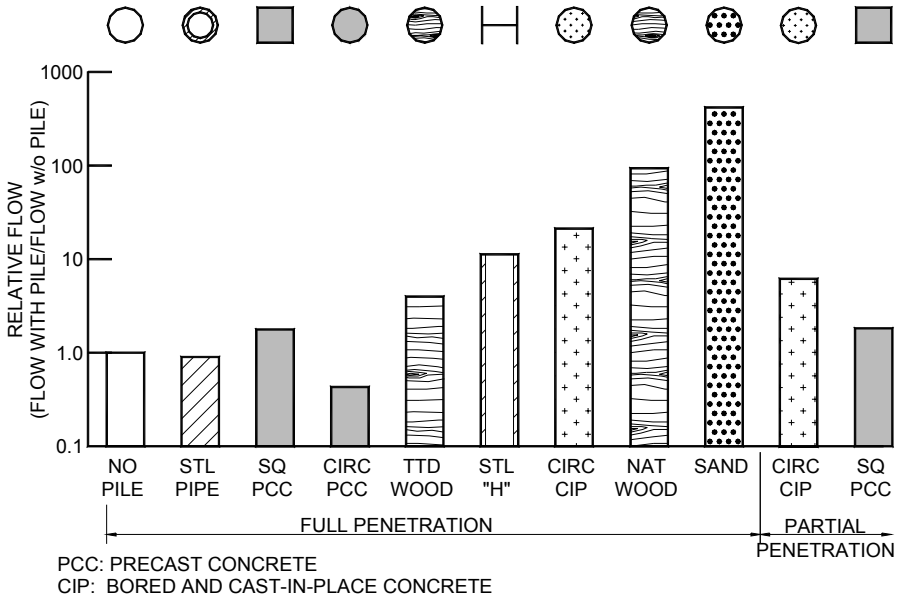

Figure 30. Relative flow for tests at UNO (Boutwell et al ., 2000 and the present investigation) [After Boutwell, et al, 2005]

The results of the tests are as follows,

1. Piles with full penetration had relative flow greater than partially penetrating piles. This was modeled by numerical studies and the analysis and results are presented in the chapter on numerical studies.
2. The cast in place cirular pile having a $L_p/L_c = 0.8$, had flow rates greater than the fully penetrating precast and cast-in-place piles. This was due to an experimental problem in the Chamber. Dye was introduced into the chamber to investigate the problem. Upon opening the chamber, it was found that the top sand layer had formed a "pathway" along the side of the chamber below the water inlet. This column formed a permeable path for the permeant to drain. The permeant drained some of the sand along with it and blocked the outlet for the outer area. The results of this chamber have to be disregarded due to this malfunction.

3. The cast in place piles had higher relative flow than the precast pile. The effect of the pile installation is discussed in the chapter on numerical studies under the lateral earth pressure considerations.
4. Square piles had more relative flow than circular piles. This difference can be attributed to "Displacement Ratio differences", which will be discussed in the chapter on Numerical Analysis under lateral earth pressure considerations.

6.2 Contaminant Transport

The contaminant transport was studied on the basis of the electrical conductivity of the brine. The changes in specific conductivity of effluent from the center, middle and outer regions were measured over time. The equation (2) was used to compute the relative concentration as discussed in Section 4. 6.2.

To determine the effect of piling on contaminant transport, a term "breakthrough time" was defined. Breakthrough time (t_b) is the time at which the specific conductivity achieved half its total change for a particular test setup.

For the no-pile case, this was defined as (T_b). The dimensionless ratio "relative breakthrough time" defined as (t_b/T_b) is a measure of the change (if any) in contaminant transport rate. A value for this parameter less than 1.0 indicates a lower breakthrough time, i.e., faster contaminant transport with the pile. A comparison of relative breakthrough times for all the tests at UNO is provided in Figure 31.

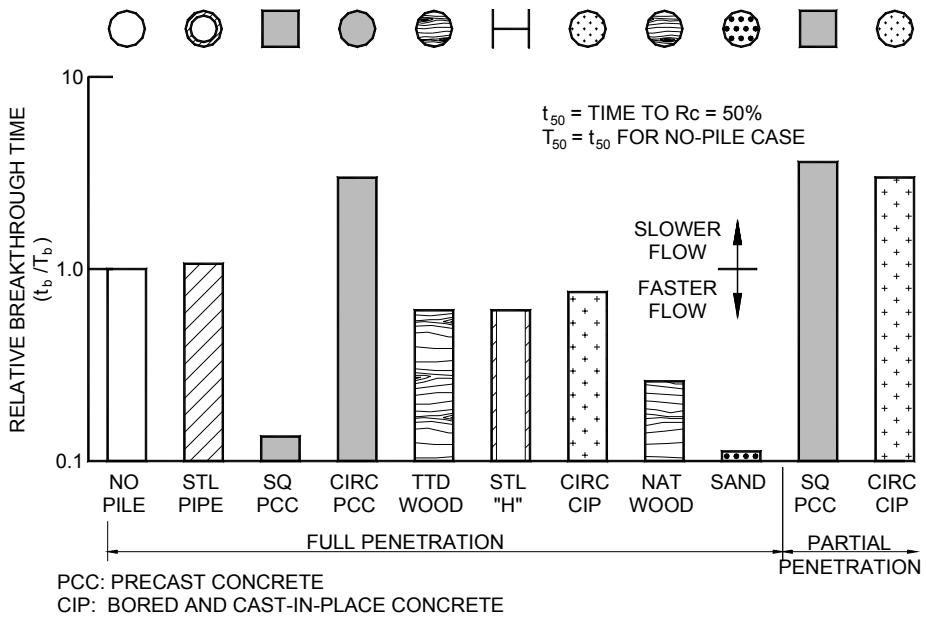

Figure 31. Relative breakthrough times for tests at UNO (Boutwell et al., 2000 and present investigation) [After Boutwell et al, 2005]

7.0 NUMERICAL STUDIES

The finite element modeling of the problem was done using the computer code SEEPS2D. SEEPS2D was developed at the Virginia Polytechnic Institute and State University. This program can be used to solve plane or axisymmetric confined or unconfined steady state seepage problems. The calibration of the program was done by modeling standard flow problems (Lambe and Whitman, 1969; Smith and Griffiths, 1998). The results were found to be in agreement with the published values. The study investigated the model chambers as two dimensional and axisymmetric steady state flow problems.

The numerical modeling was done to ascertain the effect of 1) pile permeability, 2) depth of pile embedment, and 3) pile groups on flow. To determine the effect of depth of penetration, the relative penetration (L_p/L_c) was varied. The dimensionless ratio (k_p/k_c) represents relative permeability, where k_c = permeability of the clay layer. A parametric study was conducted by varying the relative permeability from 1 to 100,000 and the relative penetration was varied from 0.5 to 1.00. The "no-pile" case has a (k_p/k_c) = 1. The top and bottom sand layers were assumed to have a permeability of 1 X 10^{-1} cm/sec, and the clay was assumed to have a permeability of 1 X 10^{-7} cm/sec (DEQ and US EPA liner standard hydraulic conductivity) .

Two-dimensional analysis was used to model the flow for chambers with square and circular piles and axisymmetric analysis was utilized to model circular piles. The ratio of diameter of chamber ($D_{chamber}$) to the diameter of the pile (D_p) is termed "relative lateral extent (R_E)". The diameter of the pile was kept constant at 2.54 cm and the diameter of the chamber was varied to obtain different values of R_E. For the model chambers, R_E = 12. For the two dimensional analysis, the R_E values used were 12, 24 and 48.

For the axisymmetric analysis, R_E was set to be 10 and 12. The effect of method of installation was not considered in this numerical study.

7.1 Two-Dimensional Analysis

The model test chamber was first modeled as a plane flow problem. The pile diameter was kept the same as the model test case. The program assumes a plane section along the chamber for analysis. The results were interpreted on the basis of "relative flow" as defined earlier. The results of the analysis are presented in Figures 32 through 35

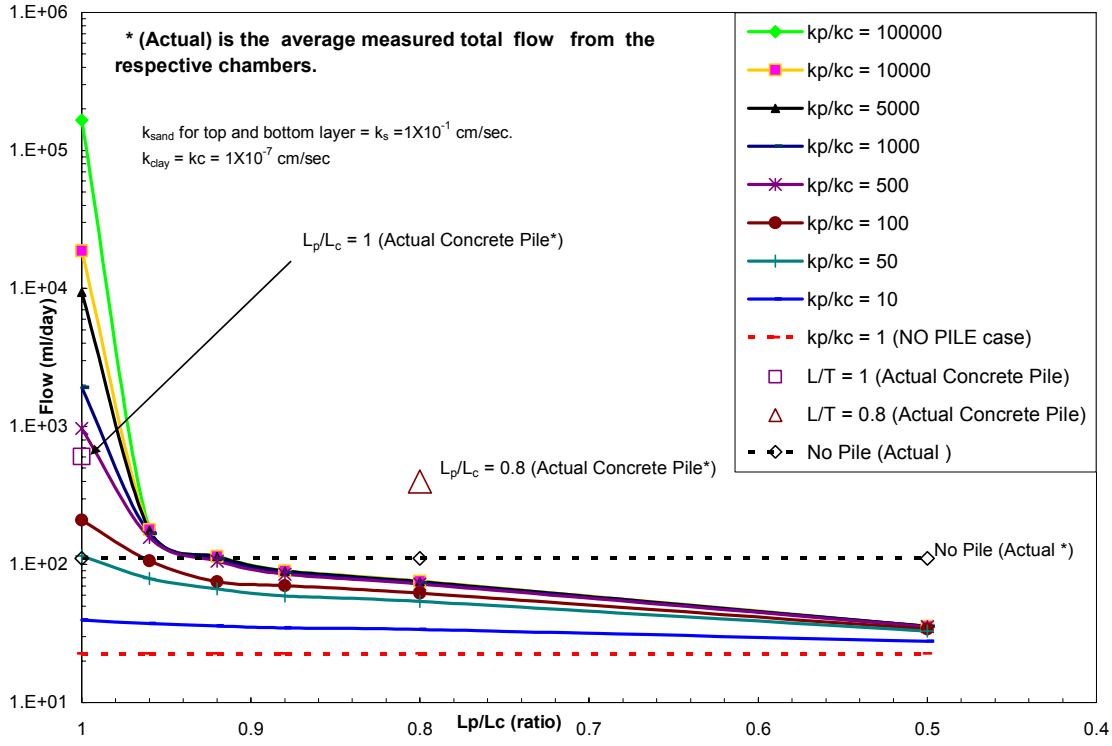

Figure 32. Plot of flow per day versus (L_p/L_c) for various (k_p/k_c): Plane Flow Analysis.

In Figure 32, the ordinate represents the average flow in ml per day and the abscissa is the dimensionless relative penetration. A logarithmic scale was chosen on the ordinate to accommodate the wide variations in the flow values.

Actual flow values obtained from the model tests are plotted in Figure 32. The variation between the actual and the plane flow analysis may be due to the program assuming a plane section along the chamber for analysis. The assumed value of permeability may also be a factor for the differences observed. The two dimensional analysis is not fully representative of the actual model tests. The plane flow analysis was conducted to model the effect of square and circular piles.

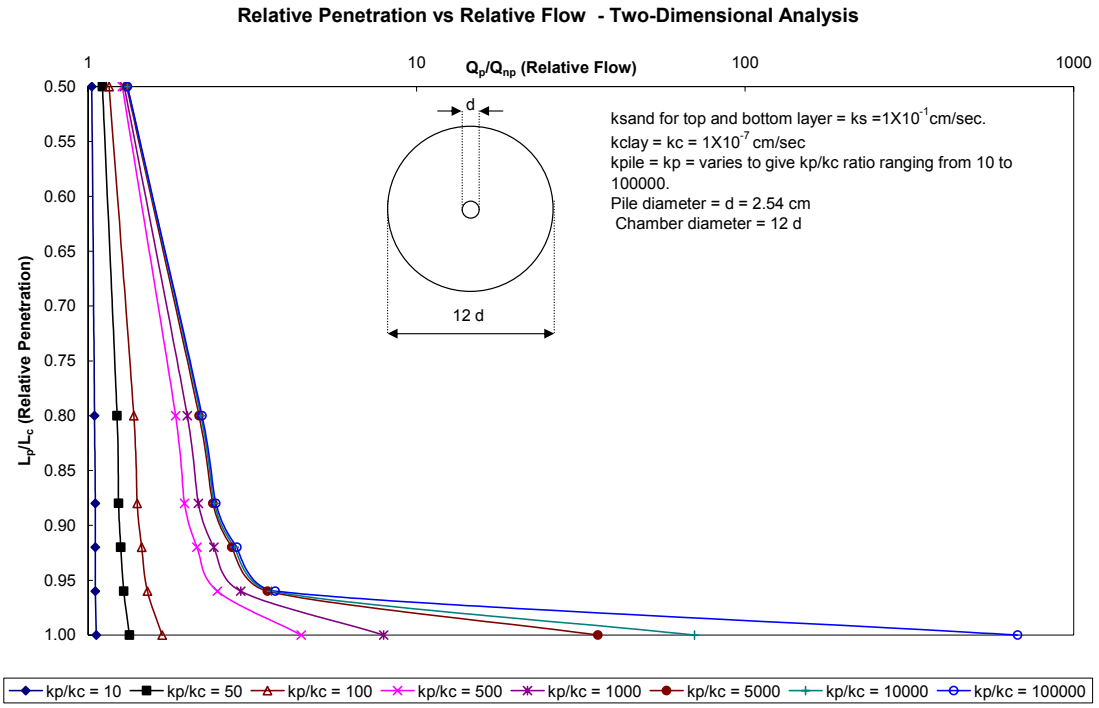

Figure 33. Relative penetration versus relative flow for the model test chamber with R_E = 12

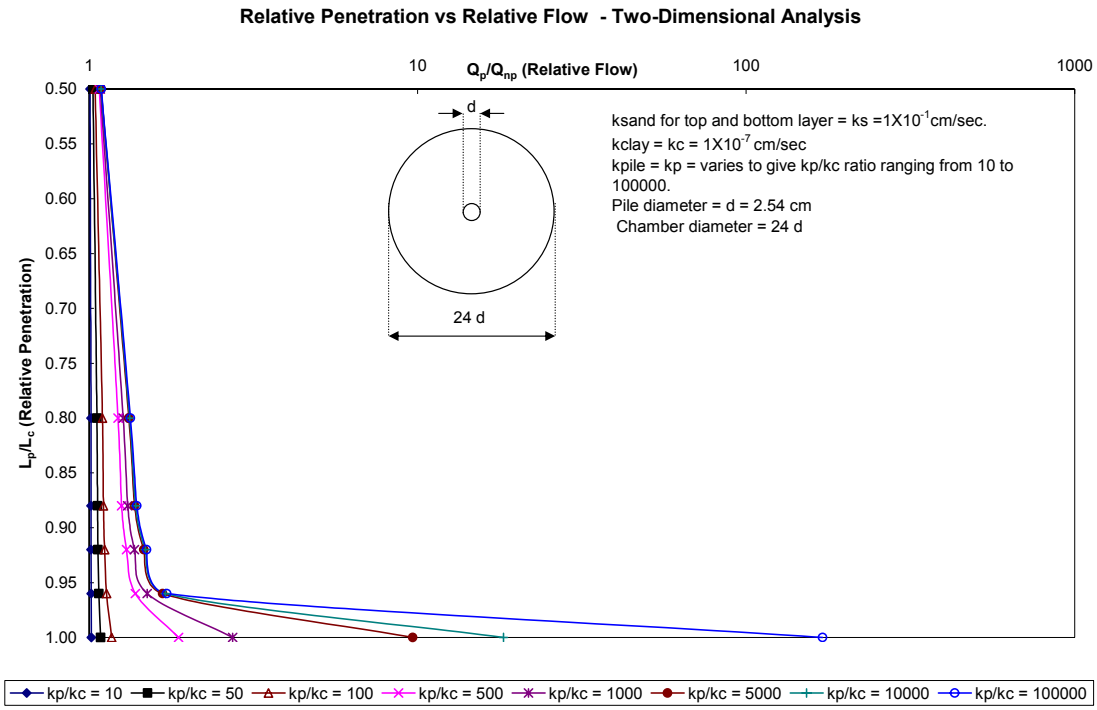

Figure 34. Relative penetration versus relative flow for a model chamber with $R_E = 24$.

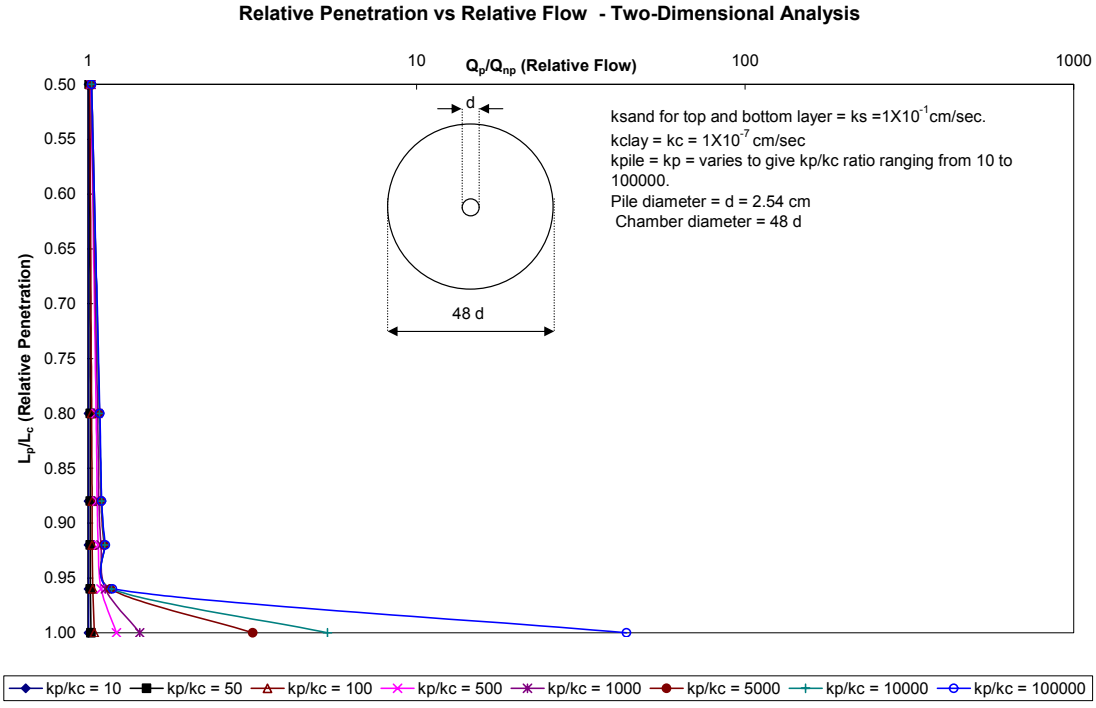

Figure 35. Relative penetration versus relative flow for a model chamber with $R_E = 48$.

Increasing in R_E reduces the relative flow. This is due to the assumption of the pile having permeability greater than the clay ($k_p/k_c > 1$). The increase in the diameter of the chamber increases the area of clay and reduces the equivalent permeability of the system. The flow rate gets reduced with increase in the relative lateral extent. Piles with a relative penetration of up to 90% exhibit an increased flow of less than ½ orders of magnitude. This is about the variability normally associated with permeability testing of natural clays and also about the same magnitude as the flow increase with fully penetrating impervious piles. The increase in relative penetration beyond 0.96 results in a considerable increase in flow, for (k_p/k_c) values greater than 1000. The maximum values of relative flow (Q_p/Q_{np}) (defined earlier in Section 6.1) is observed for full penetration of the pile ($L_p/L_c = 1$) for all values of relative permeability greater than one ($k_p/k_c > 1$).

7.1.1 Pile group analysis

To consider the performance of piles in a group, analysis was done by varying the spacing between three piles having diameters equal to the model piles. For the analysis, a section through the model chamber was simulated with three model piles spaced at 2.5 and 5 times the diameter of the model pile. The results of the analysis are presented in Figures 36 and 37.

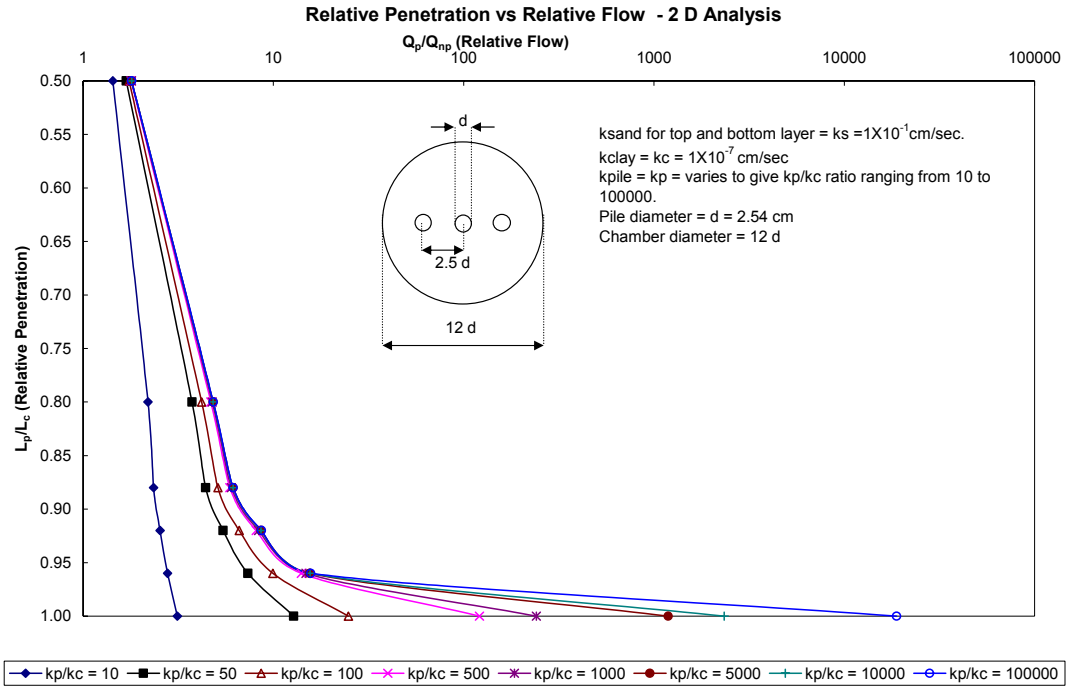

Figure 36. Relative penetration versus relative flow for a model chamber having three model piles spaced at 2.5 times the diameter of the model pile (RE = 12).

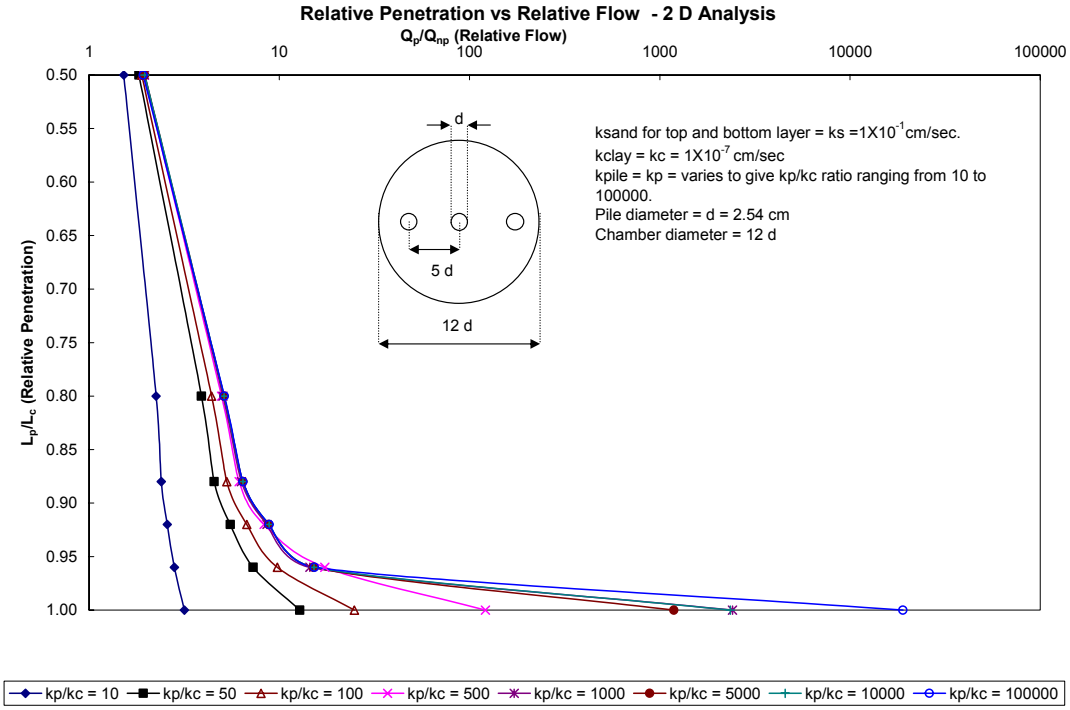

Figure 37. Relative penetration versus relative flow for a model chamber having three model piles spaced at 5 times the diameter of the model pile (R_E = 12)

The effect of relative extent was also modeled by using $R_E = 48$. The three model piles were spaced at 2.5 times and 5 times of the model pile diameter. The results of the analysis are presented in Figures 38 and 39.

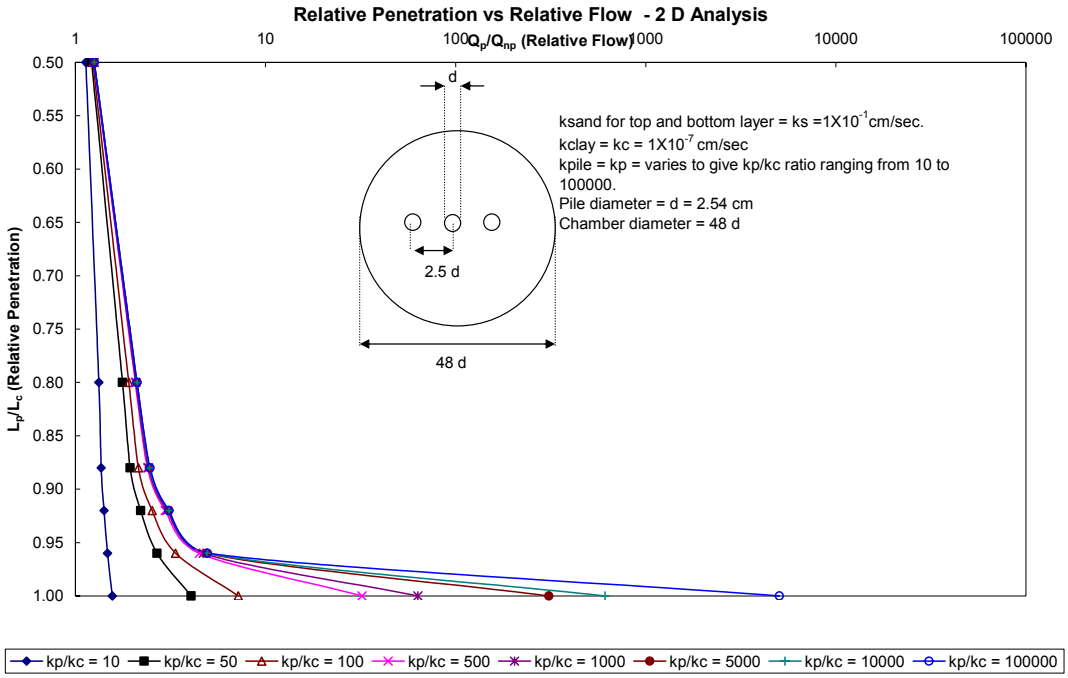

Figure 38. Relative penetration versus relative flow for a model chamber having three model piles spaced at 2.5 times the diameter of the model pile ($R_E = 48$)

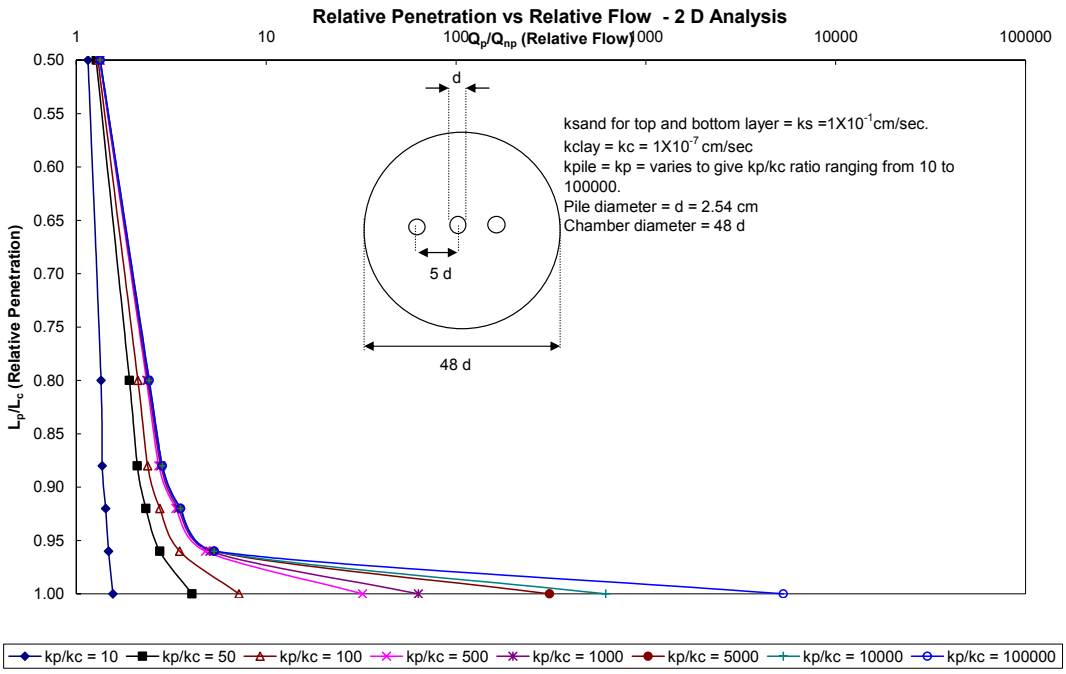

Figure 39. Relative penetration versus relative flow for a model chamber having three model piles spaced at 5 times the diameter of the model pile (R_E = 48)

7.1.2 Effect of pile spacing.

Figures 36 and 37 show that doubling the pile spacing increases the relative flow increases by 2.7 % for the most permeable case. Upon comparing the results presented in Figures 38 and 39, one observes that doubling the pile spacing increases the relative flow by 5 % for the most permeable case. As the changes in relative flow are negligible, the pile spacing can be assumed to have no significant effect on the relative flow from this analysis. The actual performance of pile groups will have to be studied by model tests to fully determine the effect of pile spacing and pile placement.

7.2 Axisymmetric Analysis

The results presented earlier considered only a plane section of the chamber applicable to circular and square shaped piles. Axisymmetric analysis was used to study the model test chamber with circular piles; a square pile can be modeled considering the equivalent circular area. The model test pile was simulated and (k_p/k_c) was varied from 1 to 100,000 similarly to the plane flow analysis. The results are presented in Figure 40. The ordinate in Figure 40 is the flow in ml/day plotted on logarithmic scale and the abscissa is the dimensionless ratio (L_p/L_c). A logarithmic scale was chosen on the ordinate to accommodate the wide variations in the flow values. The dimension less ratio (L_p/L_c) was varied from 0.5 to 1.0. Preliminary analysis indicated no significant effect on total flow for (L_p/L_c) less than 0.5; hence, values of (L_p/L_c) less than 0.5 were not considered for analysis or actual model tests.

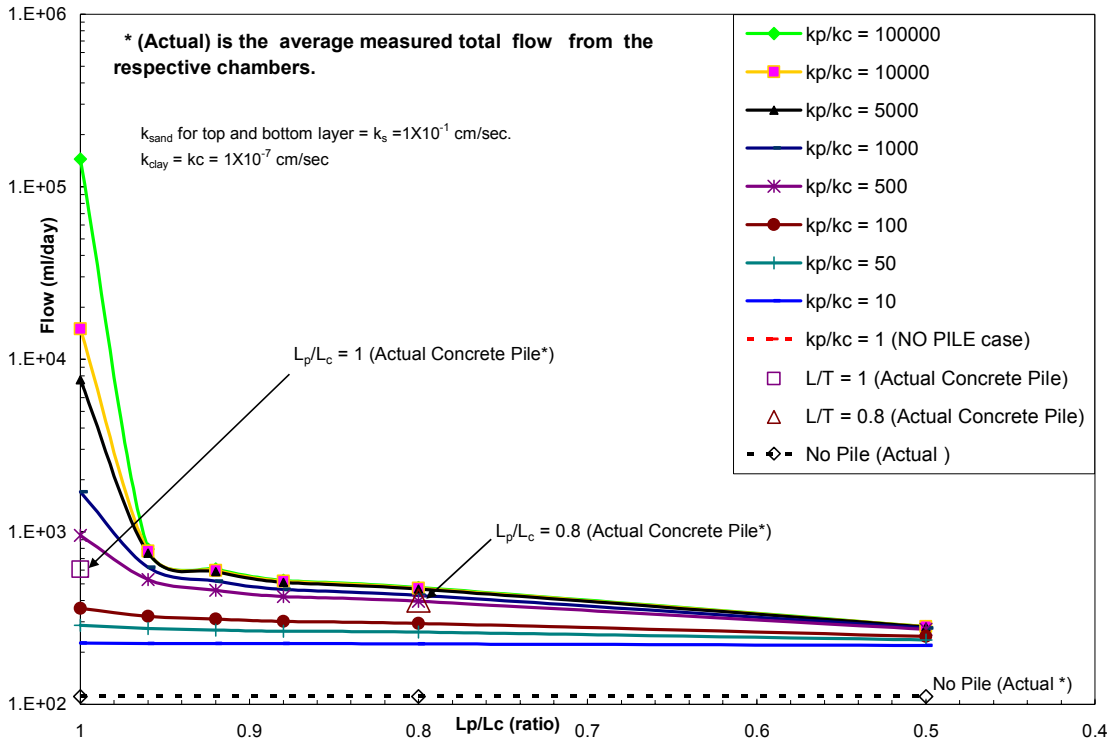

Figure 40. Plot of flow per day versus (L_p/L_c) for various (k_p/k_c).

The actual average flow rates from the chambers with water as permeant are plotted on the same plot. The actual flow rates compare well with the flow rate predicted by the program within the experimental conditions. As mentioned earlier, at about 96% relative penetration, the flow increases become considerable for (k_p/k_c) greater than 1000.

The pile group effect was modeled by considering an equivalent pile block analysis which will be discussed later.

A plot of dimensionless parameters, relative penetration (L_p/L_c) versus relative flow (Q_p/Q_{np}) is presented in Figure 41. The rate of increase of relative flow for (k_p/k_c) > 1000 is substantial. A pile which was 1000 times permeable than the clay would result in a relative flow of 8, and a pile 100,000 times permeable than the clay would result in a relative flow of 676. This indicates the threat of using long piles (high L_p/L_c) having hydraulic conductivity greater than the clay. From Figure 30, it can be seen that untreated wood pile has a relative flow of 100 and, in Figure 31 the same pile demonstrated faster contaminant transport. Permeable piles pose significant risks of pollutant migration and the rate of contaminant transport is governed by the permeability of the pile material.

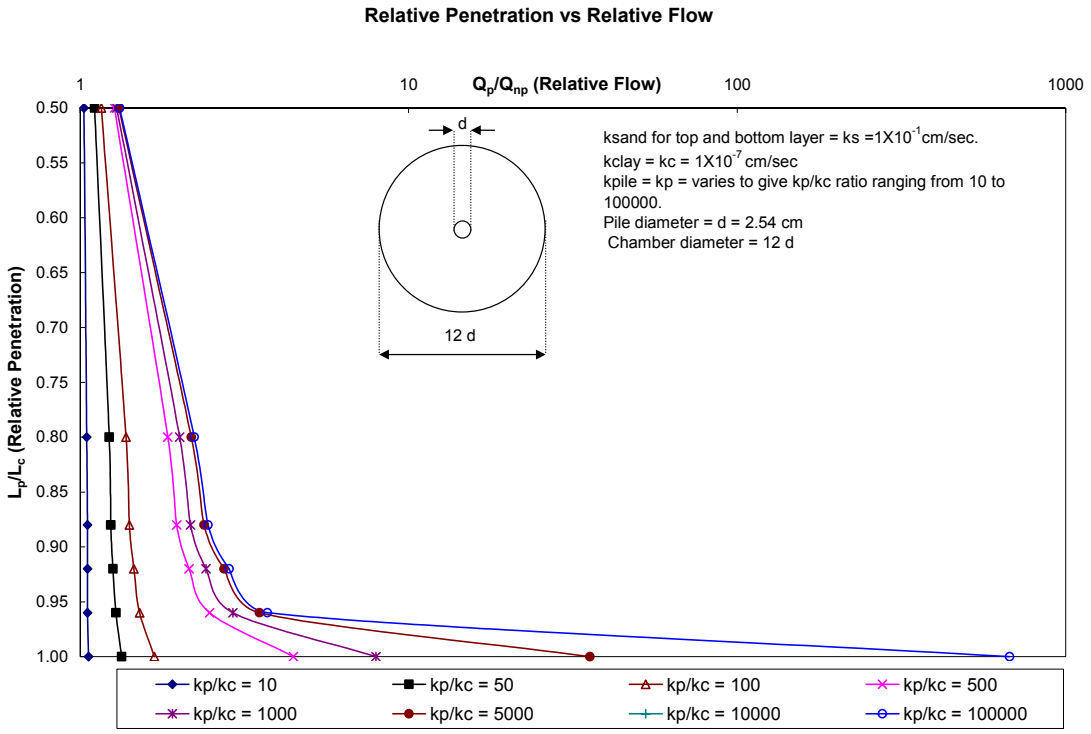

Figure 41. Relative penetration versus relative flow for the model chamber having a circular pile (R_E = 12)

The modeling was extended to a relative lateral extent of 10 to determine the effect of lateral extent.

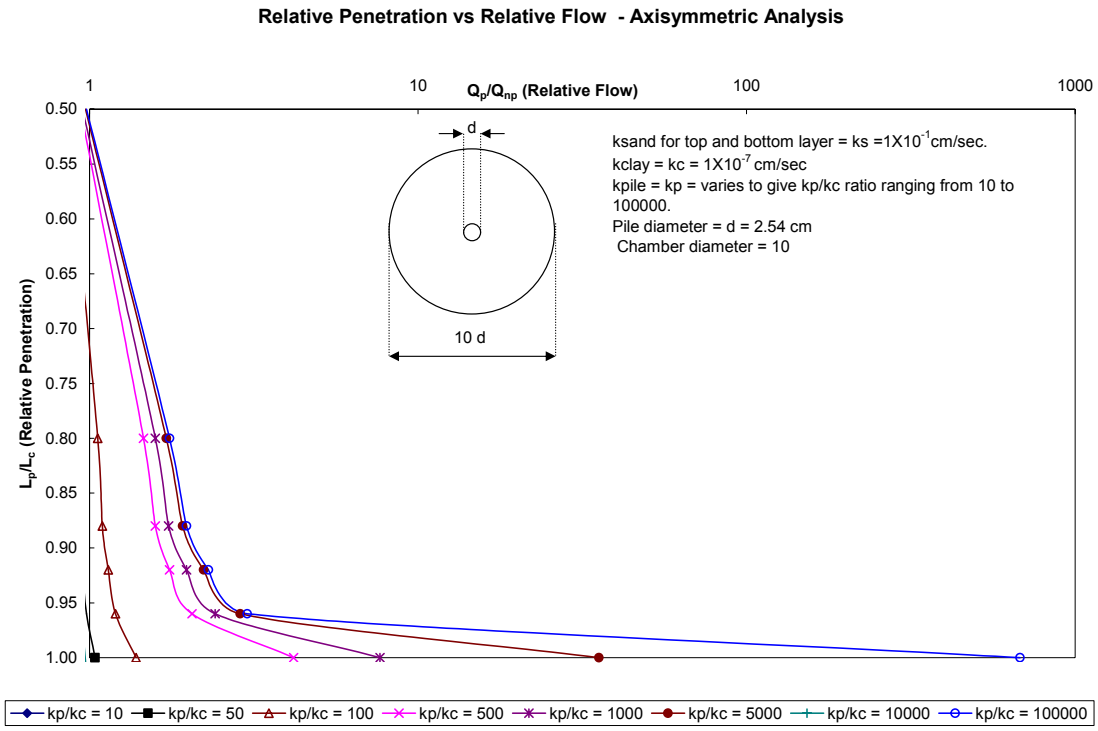

Figure 42. Relative penetration versus relative flow for the model chamber having a circular pile (RE = 10).

The finite element modeling was extended to study the effect of a pile group taken as a block. To simplify the analysis, the effect of a pile group was simulated by considering an equivalent single pile. Consider a group of nine piles of 2.54 cm diameter spaced at 6.35 cm. The total area of the block of piles is 232 cm^2. Now, the diameter of an equivalent single circular pile (d_{eqv}) can be arrived at by equating it to the area of the pile block. Hence, d_{eqv} is equal to 6.75 in (17.15 cm) if the same piles were spaced at 5 in (12.70 cm), then d_{eqv} will be 13.50 in (34.30 cm).

Figures 43 and 44 provide the results of equivalent block analysis of a pile group having piles spaced at 2.5 times the pile diameter.

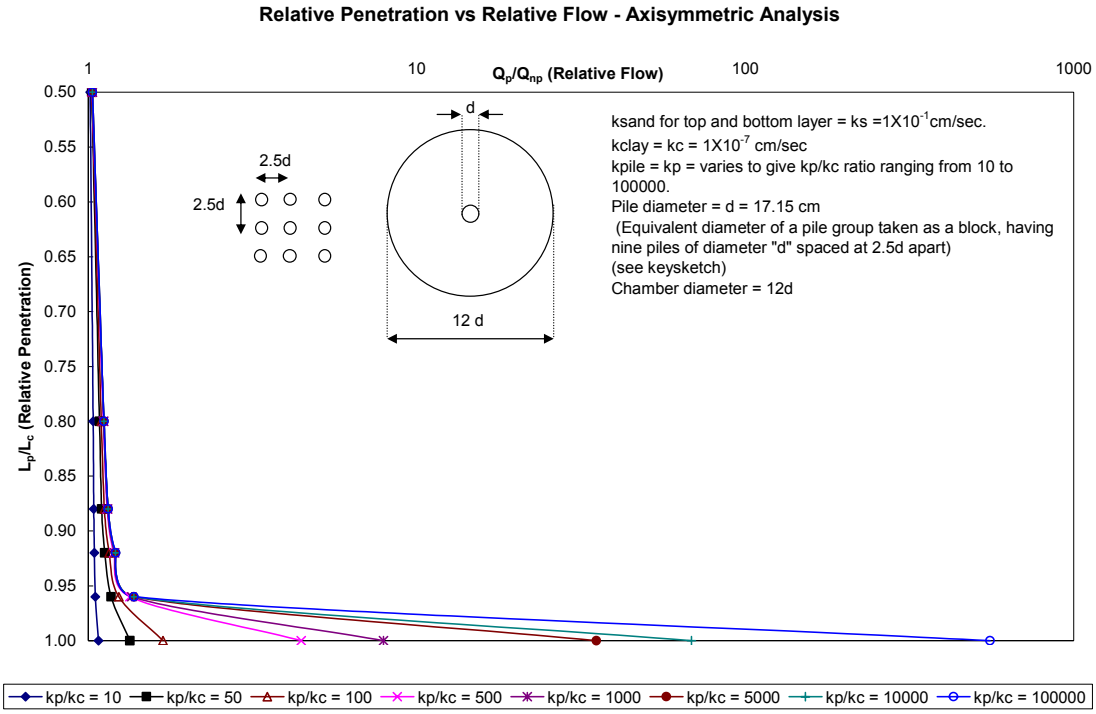

Figure 43. Relative penetration versus relative flow for the equivalent pile group case (RE = 12).

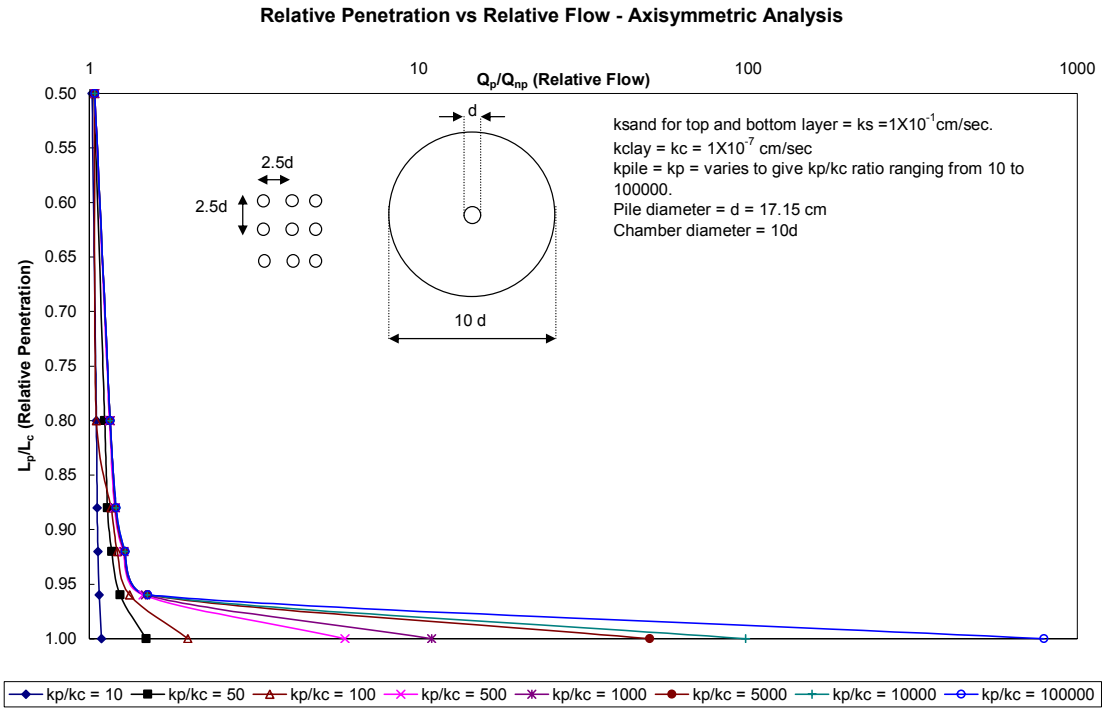

Figure 44. Relative penetration versus relative flow for the equivalent pile group case (RE = 10)

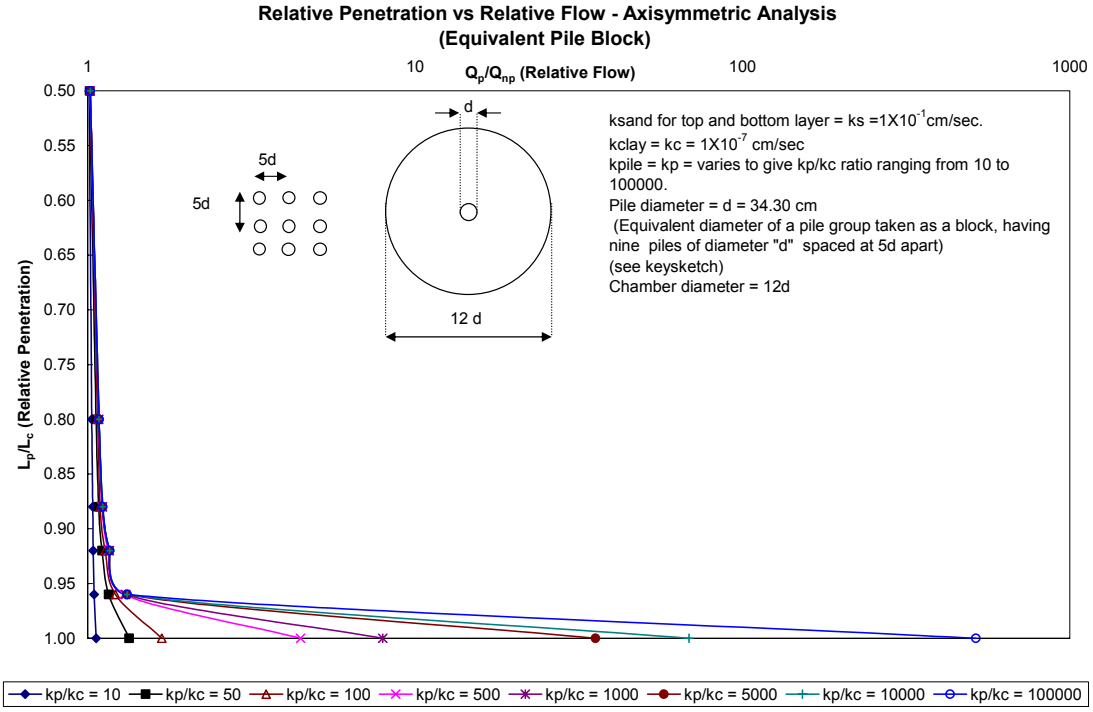

Figure 45. Relative penetration versus relative flow for the equivalent pile group case (R_E = 12).

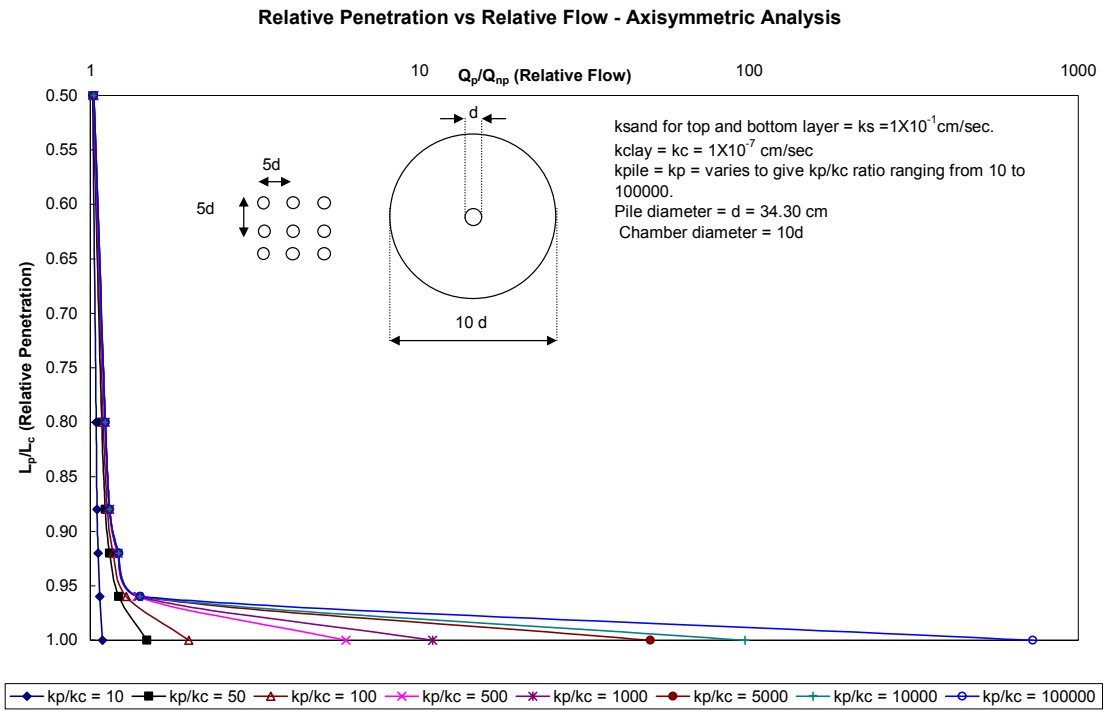

Figure 46. Relative penetration versus relative flow for the equivalent pile group case (RE = 10).

7.2.1 Effect of Relative Lateral Extent

Figures 41 and 42 indicate identical values of relative flows for all the values of (L_p/L_c) and (k_p/k_c) for the two R_E values. The relative flow values for a relative extent of 10 are slightly greater than the relative flow values for a relative extent of 12. Comparisons between Figures 40, 43 and Figures 45 and 46 indicate significant increase in relative flow with decrease in relative extent. The relative extents of 10 (Figure 44 and 46) has relative flows in excess of 43 % over the case having relative extent of 12 (Figures 43 and 45).

The effect of lateral extent on flow was modeled by plotting the relative flow against the relative permeability. Figures 47 through 52 are plots of dimensionless parameters relative flow against relative permeability for different diameters of piles and different lateral extent.

The seven plots trace the variation of the relative flow with relative permeability for different values of relative penetration.

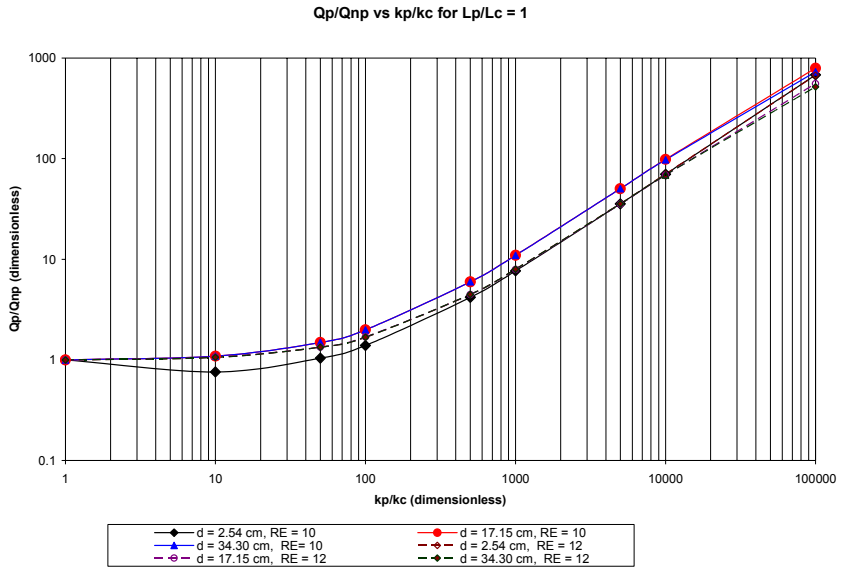

Figure 47. Relative flow versus relative permeability for Lp/Lc = 1.

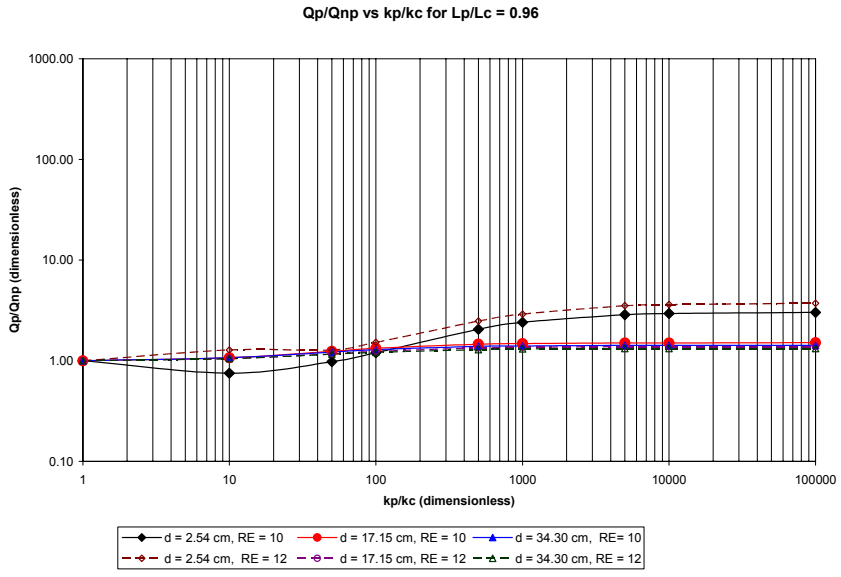

Figure 48. Relative flow versus relative permeability for Lp/Lc = 0.96.

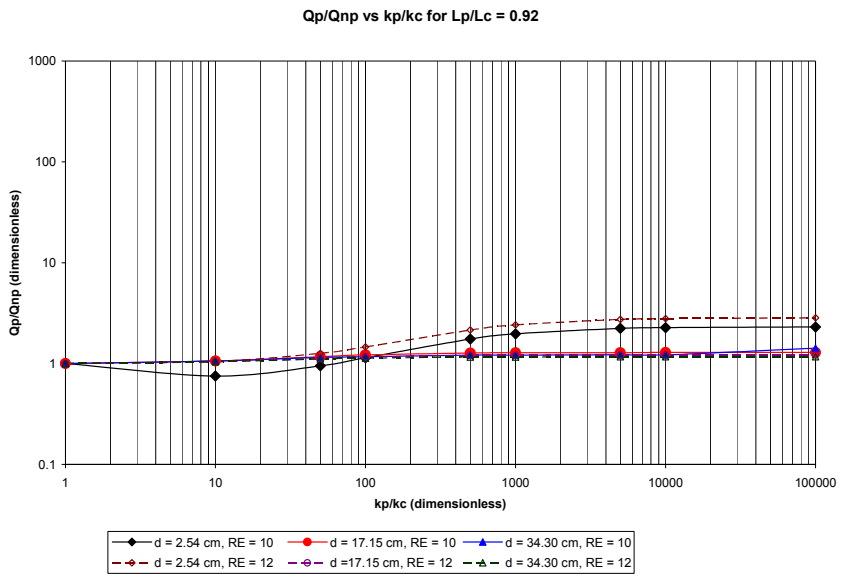

Figure 49. Relative flow versus relative permeability for Lp/Lc = 0.92.

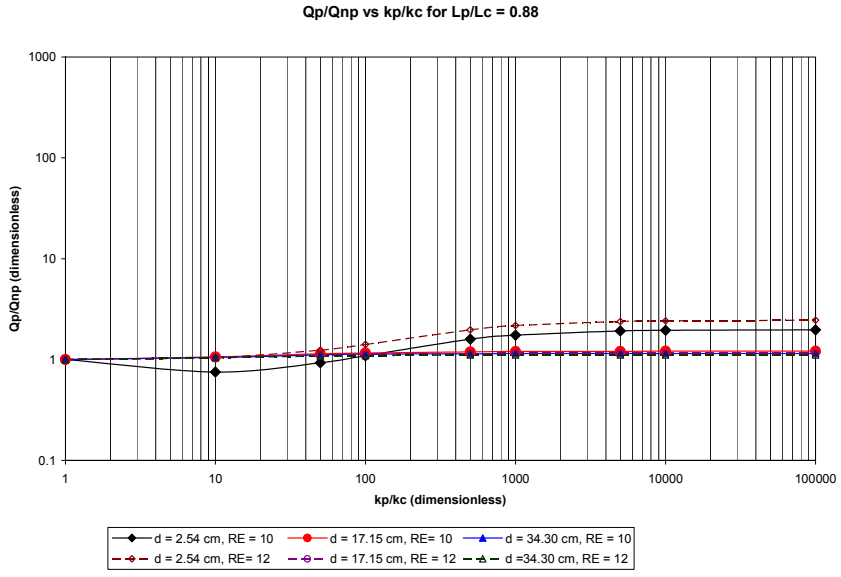

Figure 50. Relative flow versus relative permeability for Lp/Lc = 0.88.

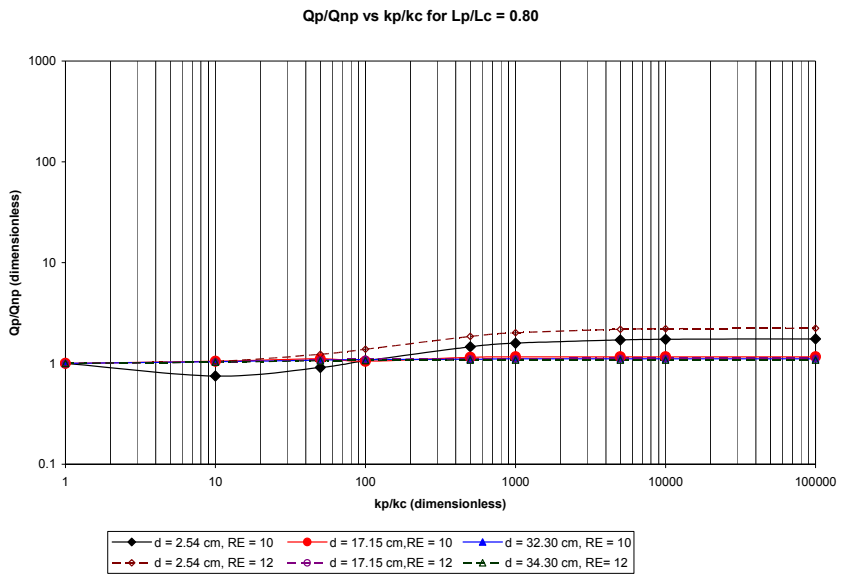

Figure 51. Relative flow versus relative permeability for Lp/Lc = 0.80.

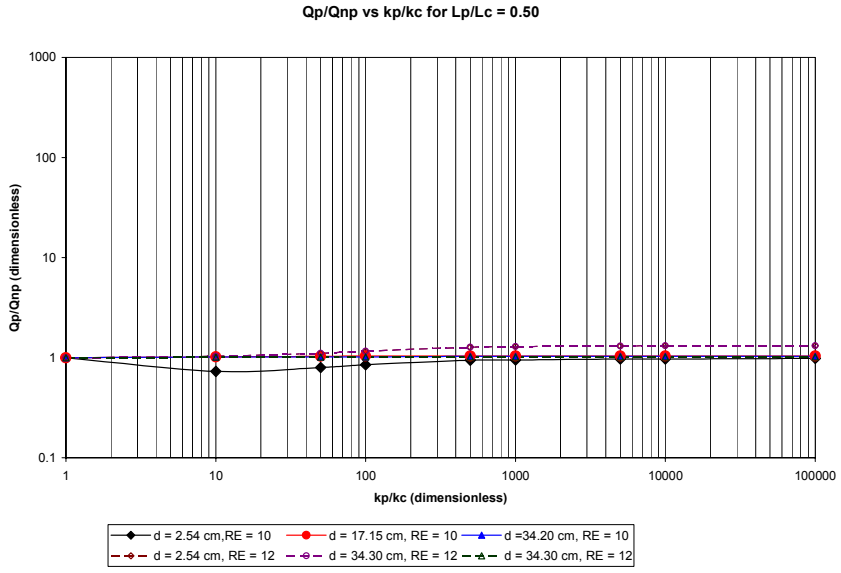

Figure 52. Relative flow versus relative permeability for Lp/Lc = 0.50.

From Figure 47, relative flow increases with relative permeability for $(L_p/L_c) = 1$. Figures 48 to 51, indicate a point of contraflexure at a relative permeability value of 100. From Figure 48, the curve for a pile having a diameter of 2.54 cm and relative extent of 10 traces a concave path until it reaches a relative permeability of 100.

Then the curve changes the trend and increases in a convex path. From the same plot, a similar pile having a relative extent of 12 traces a convex path, shows a dip at relative penetration of 100 and then continues with a concave trend and finally has a higher relative flow than its counterpart having a relative extent of 10. This leads to some uncertainty with respect to the effect of lateral extent. A threshold value of relative permeability can be obtained by determining the value of relative permeability that leads to minimum flow.

7.3 Conclusions from Numerical Analysis.

The results of the numerical analysis compared well with the results of the model tests within experimental limitations. The numerical model predicted higher flow rates for piles fully penetrating the clay layer; the same was observed with fully penetrating model pile tests. With the increase in pile permeability the flow rate increased along with the rate of contaminant transport. This was experimentally observed by the model tests on untreated wooden piles (Boutwell et al, 2001; McManis et al, 2002).

In practice, common pile group spacings are 5 diameters or less. From the pile group analysis, a 3-pile group increased the rate of flow relative to the ideal single pile case by a factor of 2.70 for the assumed most permeable pile case (k_p/k_c = 100000). This indicates that cumulative flow from a 3 pile group is less than 3 times the flow from a single pile. Since the disturbed (plastic) zone around each pile extends out at least 2 pile diameters beyond the pile, the zones will normally overlap. Thus, the area available for flow from each pile in a group is less than that for a single pile. The overall flow must therefore be less than the single pile flow times the number of piles in the group. For all (k_p/k_c) ratios, the group flow ranges from about 20% (at L_p/L_c = 0.5) to 90% (at L_p/L_c = 0.9) of the cumulative single pile flows.

The plane flow analysis predicted a negligible increase in flow with increase in pile spacing for the assumed most permeable pile case.

8. CAVITY EXPANSION THEORY APPLIED TO MODEL TESTS

8.1 Conduit Formation

The threat of conduit formation for contaminant transport was discusses in section 4.1.2. Several physical mechanisms exist which seal such an annulus or any other disturbance around the pile. O'Neill and Reese (1999), suggest that drilled cavities (shafts) without excavation support pose no risk of collapse until the excavation depth is less than about 5 C_u/γ. C_u being the undrained shear strength at failure and γ is the total unit weight of the soil. For a water filled hole, γ is to be replaced by γ', which represents the buoyant unit weight of soil. The potential for soil collapse is substantial for under-consolidated clay deposits, possible in normally consolidated clay deposits and minimal for over consolidated clays. This has been confirmed by the field observations of excavations on sites with artesian conditions in all three types of clays (Boutwell et al, 2005).

8.2 Lateral Earth Pressure Considerations

For driven piles, lateral earth pressure is the dominant sealing method. The lateral earth pressures against a driven pile are normally computed using cavity expansion theory (Ladanyi, 1963; Vesic, 1972; Massarch, 1978; Carter, et.al., 1986; Alfaro and Wong, 2001).

As a pile is driven into the ground, the soil around the pile undergoes shear distortion and the soil below the pile experiences compression distortion. Additional distortion occurs as the pile advances due to sliding friction. The soil around the pile gets pushed laterally to locations at or beyond the pile radius (r_u). At some distance "r_p" the plastic zone is delineated from the elastic zone. "r_p" represents the radius of the plastic zone. The stored elastic stress in both elastic and plastic zones will force the soil against the pile. Figure 53 depicts the plastic zone and the elastic

zone along with the potential vertical cracks; (p_{max}) represents the maximum expansion pressure that the soil around the pile can develop.

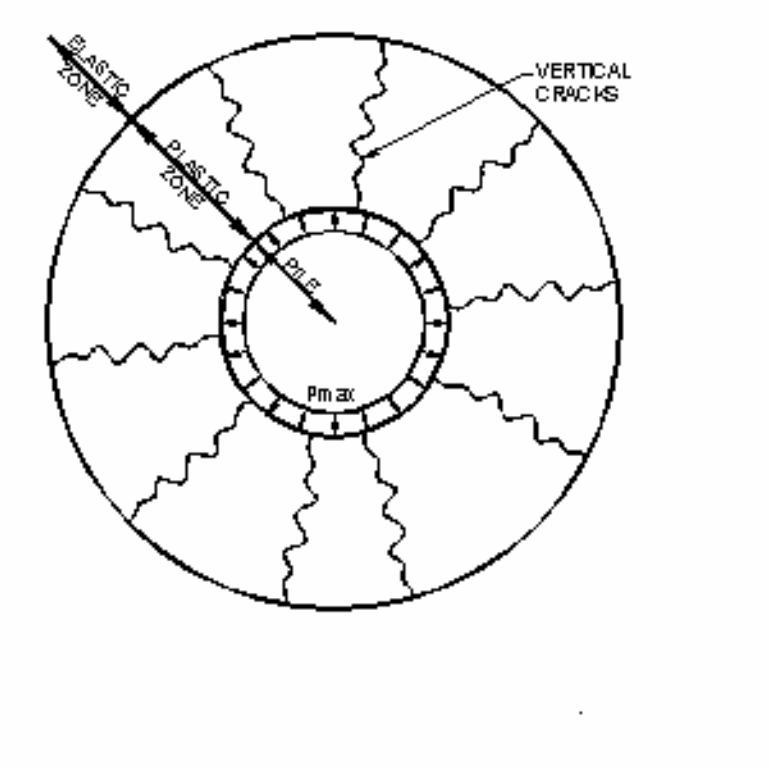

Figure 53. Plasic zone around the pile (Boutwell et al., 2005)

Bearing capacity theory indicates that in clays ($r_p/r_u = 4$), while cavity expansion theory suggests that ($r_p/r_u = 6$ to 8). A parametric study was conducted to determine (r_p/r_u) by varying the dimensionless ratio (E/C_u) from 1 to 300, where E = Young's modulus of soil. The dimensionless ratio (r_p/r_u) was found to vary from 0.62 to 10.72 and had an average value of 6.87.

The expansion pressure due to a cavity of equivalent diameter as the model pile was computed assuming values of undrained shear strength of clay. The undrained shear strength of clay was assumed to be 2.60 psi (0.12 kN/m^2) for soft clay, 5.20 psi (0.25 kN/m^2) for medium clay and 10.40 psi (0.50 kN/m^2) for stiff clay.

The ratio (E/Cu) was varied from 100 to 450. The results of the analysis are presented in Figure 54. In Figure 54, expansion pressure is plotted against the dimensionless parameter (E/Cu). It is seen that the expansion pressure is relatively greater for stiff clays than for soft and medium clays.

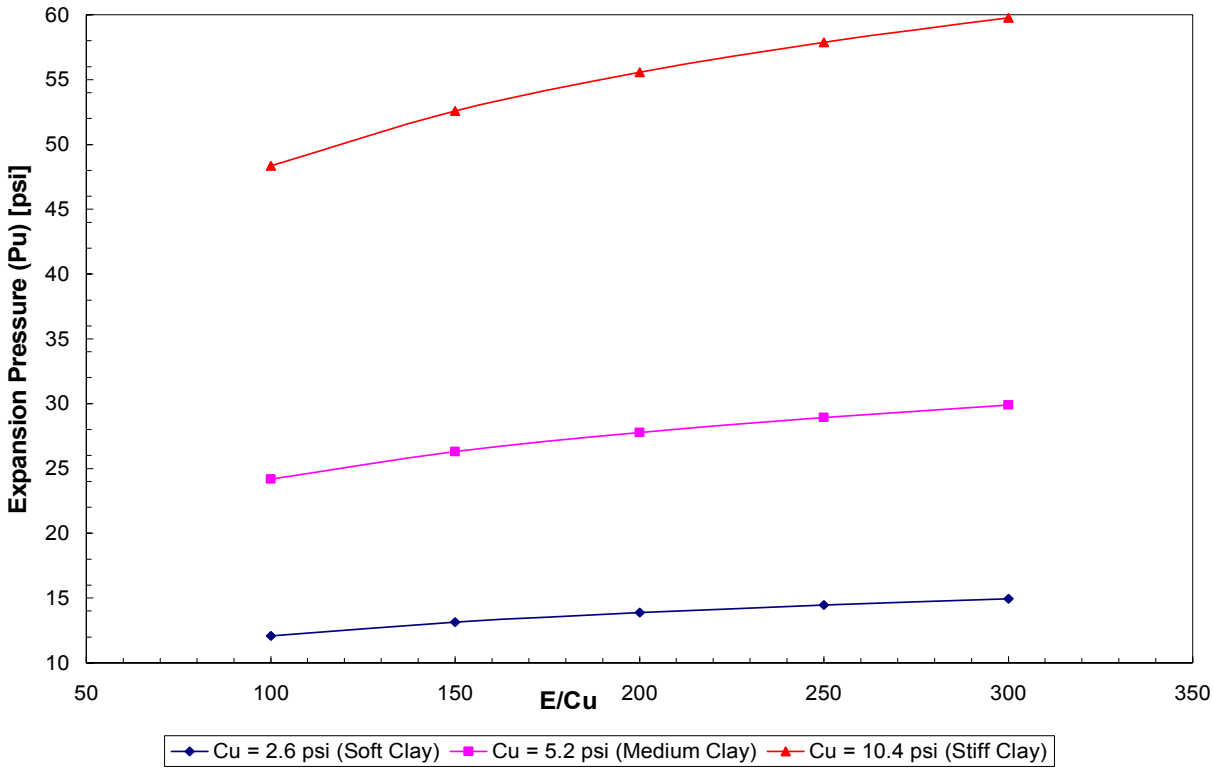

Figure 54. Expansion pressure versus E/C_u for soft, medium and stiff clays.

According to Massarch (1978), during pile driving in clay, vertical cracks are formed around the pile in the plastic zone. These cracks can serve as potential drainage channels and significantly increase the potential for contamination. However, Massarch (1978) also states that cracks close within four hours after pile driving as the excess pore water pressure due to pile penetration dissipate.

8.3 Displacement Piles

The ultimate lateral pressure developed (p_u) is independent of the radius of the pile. Displacement piles may provide a better sealing if the ratio of unit volume of the pile to the external surface area is high. "Displacement Ratio" (R_d) is the ratio of the cross-sectional area of the pile to the area of a square enclosing its outside perimeter. This is a measure of soil displacement. For example, a solid square pile would have (R_d = 1.00), a round solid pile (R_d = 0.79), and a typical "H"-pile about (R_d = 0.12). Data in Hannigan, et.al.(1996) indicates that piles with high (R_d) do develop greater lateral pressures during driving then those with low (R_d). Further, the degree of lateral pressure increase indicated in that publication is relatively small; a 30% increase in pressure for a square pile over an "H"-pile. The lateral pressures developed by a tapered pile can be significantly greater relative to straight sided piles. The lateral pressure developed by a pile with a taper of 0.45 cm per meter is 50% to 100% greater than that developed by a similar straight-sided pile (Hannigan, et.al, 1996).

8.4 Bored Piles.

In the case of bored piles, apart from the lateral pressure exerted by potential soil collapse, no other lateral pressure is available at the pile-soil interface. The fluid pressure exerted by concrete is sufficient to ensure a seal of the pile-soil interface. The potential for formation of vertical cracks is minimal. The radial pressure exerted by bored piles is lesser than that exerted by driven piles but can be considerable. In practice, grouting has been extensively used for sealing boreholes and groundwater monitoring wells on contaminated sites. The empirical evidence suggests that the fluid pressure may be sufficient to provide sealing at the pile/soil interface.

9. SUMMARY AND CONCLUSIONS

The results of model tests and numerical studies are presented. The model tests results indicated potential for contaminant transport for selected pile cases. There are several factors which govern the contaminant transport due to pile foundations in Brownfields. The established mechanisms of contaminant transport include

1) Direct Transfer

2) Conduit formation

3) Wicking and

4) Chemically treated piles.

Depth of penetration plays a significant role in contaminant transport. The model tests and numerical studies indicate less potential for contaminant transport for relative penetrations less than 0.95. Partial penetration may not be a economically viable option due to the reduced bearing capacity.

Square shaped piles had higher potential for contaminant transport than circular piles.

Cast-in-place piles were found to have greater potential for contaminant transport relative to driven piles.

Recommendations based on the previous investigation (Boutwell et al., 2000 and McManis et al., 2002) and the current study to minimize contaminant transport due to pile foundations in Brownfields includes:

- Use of clean piles (Without chemical treatment or contamination)
- Use of low-permeability piles
- Use of displacement piles.
- Use of piles with a conical tip

10. REFERENCES:

Alfaro, M. C., and Wong, R. C. K., (2001). *"Laboratory Studies on Fracturing of Low-Permeability Soils,"* Canadian Geotechnical Journal., Vol. 38., 303-315.

Baetsle, L.H. (1969). Migration of radionuclides in porous media. In: *Progress in Nuclear Energy Series XII*, Health Physics, A. M. F. Duhamel (Ed.), Pergamon Press, Elmsford, NY, 707–730.

Boutwell, G.P., Nataraj, M.S and McManis K.L.,(2000). "*Deep Foundations on Brownfields Sites*", Prague 2000, Proceedings of the 5th Conference on Environmental Problems in Eastern Europe, Prague, Czech Republic.

Boutwell, G.P., Nataraj, M.S. and McManis, K.L.,(2001), "Pile Foundations: An Environmental Problem?" The Louisiana Engineer, Journal of the Louisiana Section, ASCE., Vol. 9, No. 2., 5-24.

Boutwell, G.P., Nataraj, M.S., McManis, K.L., & Satyamurthy, R., (2005), "Installation of Driven Piles in Brownfields Sites", *2005 Pile Driving Contractors Association Winter Roundtable*, Charleston, SC.

Carter, J. P., Booker, J. R. and Yeung, S. K., (1986), *"Cavity Expansion in Cohesive Frictional Soils,"* Geotechnique, 36(3)., 349-358.

Coduto, D.P., (2001), "*Foundation Design Principles and Practice"*, Second Edition, Prentice Hall., 383-384.

Das, B.M., (1999), "*Principles of Foundation Engineering",* Fourth Edition, PWS Publishing, 578.

Dunn, R.J., (1995), *"Design and Construction of Foundations Compatible with Solid Wastes,"* ASCE Geotechnical Special Publication No. 53, American Society of Civil Engineers, New York, NY., 139-157.

Environment Agency, "*Piling and penetrative ground improvement methods on land affected by contamination: Guidance on pollution prevention,"* NGWCLC Report NC/99/73, 2000.

Green, W.A. and Ampt, G.A., (1911), "Studies on Soil Physics,1, The Flow of Air and Water through Soils", *J.Agr.Sci,4,*1-24.

Hannigan, P. J., Goble, G. G., Thendean, G., Likins, G. E and. Rausche, F, (1996), Design and Construction of Driven Pile Foundations, USDOT Federal Highway Administration, Washington, D.C., 9.30-9.35.

Hayman, J. W., R. B. Adams, and R. G. Adams, (1993), *"Foundation Piling as a Potential Conduit for DNAPL Migration,"* Proc. Air & Waste Management Association Meeting, Denver, CO, June, 1993.

Kamon, M.T., Katsumi, T., Inui, T., and Hamada, S., (2005), "*Environmental Acceptability of the installation of Piles Through the Bottom Clay Barrier at Costal Landfill Sites,"*ASCE Geotechnical Special Publication No.142, ASCE, Reston, VA.

Ladanyi, B., (1963), "Expansion of a cavity in a Saturated Clay Medium", Journal of Soil Mechanics and Foundations Division, ASCE, Vol.89, No.SM4, Proc. Paper 3577, 127-161.

Lambee, T.W and Whitman, R.V.,(1969), "Soil Mechanics", John Wiley and Sons, New York.

Massarch, K. R., (1978), *"New Aspects of Soil Fracturing in Clay,"* Journal of the Geotechnical Engineering Division, American Society of Civil Engineers, Vol. 104, No. GT8 ., 1109-1123.

McManis, K.L, Nataraj, M.S, Boutwell, G.P and Achlietner, S. (2002), "*Deep foundations in Grayfields"*, Schlieder Urban Environmental Systems Center, University of New Orleans., Research report No.2002-1.

Meyerhof, G.G.,(1961), "*The Ultimate Bearing Capacity of Wedge-Shaped Foundations*", Proc. Fifth Int. Conf. on Soil Mechanics and Foundations Paris, France, A.A. Balkema Publishers, Vol. 2, pp. 105-109.

Nataraj, M.S, McManis, K.L, Boutwell, G.P, and Satyamurthy, R. (2004). "*Deep foundations in Brownfield Areas: A Continuing Investigation",* Schlieder Urban Environmental Systems Center, University of New Orleans.,*Research* Report No. 2004-01.

O'Neill, M.W., and Reese, L. C., "Drilled Shafts: Construction Procedures and Design Methods", FHWA-IF-99-025, International Association of Foundation Drilling, ADSC-TL-4, Dallas, TX, p. 37.

Smith, I.M and Griffiths, D.V. (1998), "Programming the finite element method", 3rd Edition, John Wiley and Company, New York.

Terzaghi, K., (1943), *Theoretical Soil Mechanics,* Wiley, New York.

US EPA (2002)., Proposal Guidelines for Brownfields Assessment, Revolving Loan Fund, and Cleanup Grants - Appendix 3. Guidance on Sites Eligible for Brownfields Funding Under CERCLA §104(k).

US EPA (2003)., "Reusing Land and Restoring Hope:
A Report to Stakeholders from the US EPA Brownfields Program".

Vesic, A. S., (1972), *"Expansion of Cavities in Infinite Soil Mass,"* Journal of the Soil Mechanics and Foundations Division, Am. Soc. Civil Engineers, Vol. 98, No. SM3., 265-290.

APPENDIX I

Co-relation of Electrical Conductivity measurements and NaCl content.

I .For the first phase:

The degree of contamination of the drained water is determined by measuring its electrical conductivity. Calibration tests were performed to find the Na-Cl content for the measured conductivity readings in the tests. The test was performed with a probe directly connected to one of the monitors. Different known concentrations of NaCl (0, 5, 7.5, 10 and 12.5, 15 g/L) were tested. A sample of the solution was put in a 30-mL beaker. Conductivity was measured by inserting the probe. The results of this calibration test for the first phase of tests are presented in Figure i.

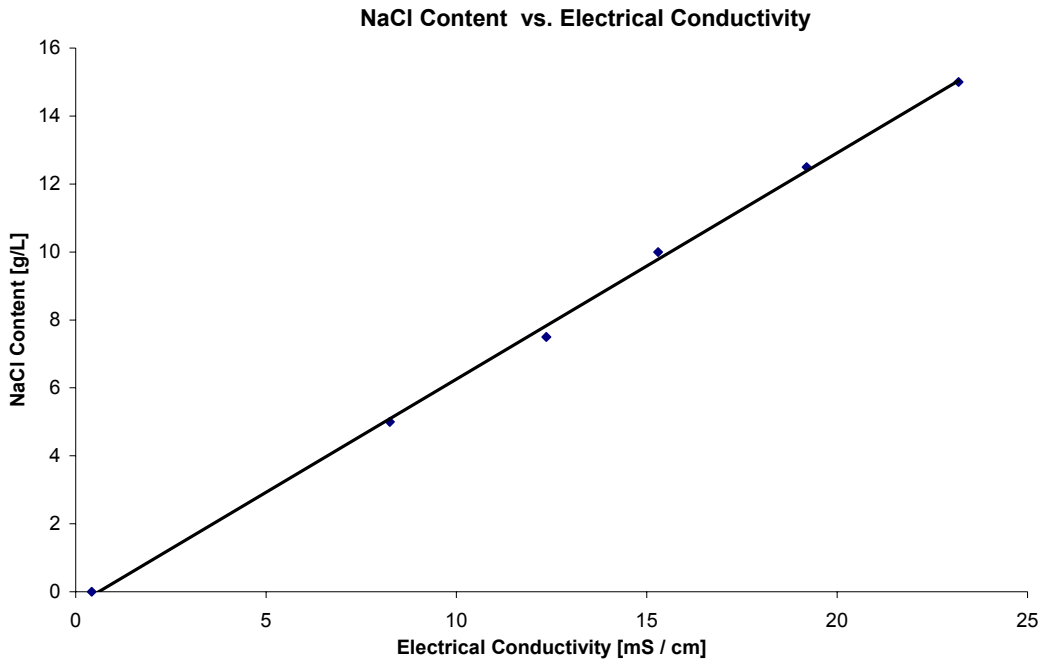

Figure i - NaCl Content in drained fluid as a function of its electrical conductivity (After McManis et al., 2002)

.

The relationship between measured electrical conductivity [mS /cm] and the actual concentration of NaCl [g/L] is given as:

$$NaCl\ [\mathrm{g / L}] = EC\ [\mathrm{mSiemens\ / cm}] \cdot 0.6588\text{-}0.2767$$

where

C_{NaCl} [g/L] = Concentration of NaCl

EC_{NaCl} [mS/cm] = Electrical Conductivity of drained fluid [milliSiemens/cm]

II. For the second phase:

Calibration tests were conducted for the second phase as described in Section I. The results are presented in Figure ii.

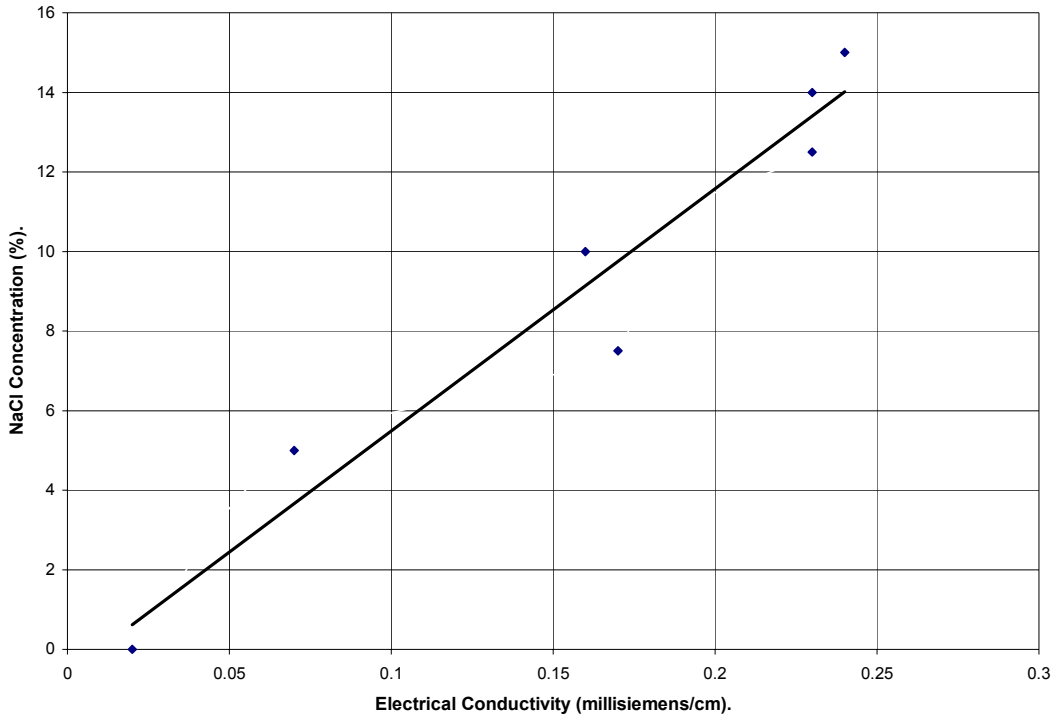

Figure ii . NaCl Content in drained fluid as a function of its electrical conductivity. (After Nataraj et al., (2004)).

APPENDIX II

I. One dimensional Green-Ampt model:

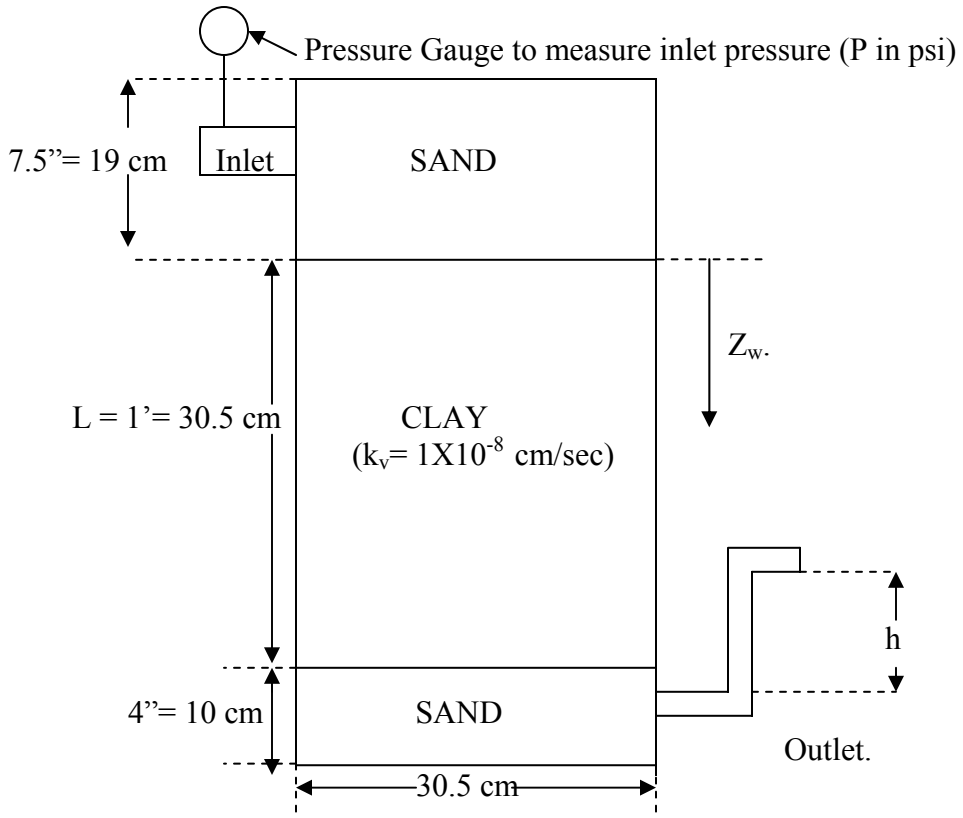

Figure (a) . Schematic representation of a cross section of test chamber.

Following are the values of the various parameters used in the calculation,

1. γ_d = 106.40 pcf.
2. ω_0 = 16.5 %
3. G = 2.7
4. Ψ = 0 cm
5. K_v = 1x 10^{-8} cm/sec.
6. H = (P*70.4 + L – h)

   = (15*70.4 + 30.5 - 10.16) = 1076.34 cm.

where,

γ_d = maximum dry density of the clay sample (pcf)

ω_0 = moisture content used to achieve γd for the clay sample (%)

G = specific gravity of clay

H = applied head (cm). L = thickness of clay layer = 30.5 cm.

P = pressure head measured at the inlet (psi) **[Note: 1 psi = 70.4 cm of water].**

h = pressure head measured at the outlet (cm)

I.1 Sample computations:

I.1.1 Data for Computation:

1) γ_d = 106.40 pcf. (16.72 kN/m^3).
2) ω_0 = 16.5 %
3) G = 2.7
4) Ψ = 0 cm (0 in)
5) K_v = 1X 10^{-8} cm/sec. (4 X 10^{-9} in/sec).
6) H = (P*70.4 + 30.5 –h)

   = (15*70.4 + 30.5 -10.16)

   = 1076.34 cm. (423.75 in)

I.1.2 Calculation of n_a:

$$n = \left(1 - \frac{\gamma_d}{G\gamma_w}\right)$$

$$n = \left(1 - \frac{106.40}{(2.7)(62.4)}\right)$$

n = 0.37

$$s = \frac{\omega_0}{\frac{\gamma_w}{\gamma_d} - \frac{1}{G}}$$

$$s = \frac{0.165}{\frac{62.4}{106.40} - \frac{1}{2.7}}$$

s = 0.76

n_a = n (1-s) = 0.37 (1- 0.76) = 0.09.

I.1.3 Calculation of H'

$$H' = H\left(1 + \frac{\psi}{H}\right)$$

$$H' = 1076.34\left(1 + \frac{0}{1076.34}\right)$$

H' = H = 1076.34. (423.75 in)

I.1.4 Calculate (t) for various (Z_w):

$$t = \left(\frac{n_a H'}{K_v}\right)\left[\frac{Z_w}{H'} - \ln\left(1 + \frac{Z_w}{H'}\right)\right]$$

(Note: The value of t obtained from the above computation is in seconds. To convert it into days the relationship used is 1 day = 0.864 x 10^5sec)

For Z_w = 5 cm,

$$t = \left(\frac{(0.09)1076.34}{1e-8}\right)\left[\frac{5}{1076.34} - \ln\left(1 + \frac{5}{1076.34}\right)\right]$$

t = 104337 sec = 1.2 days.

For Z_w = 10 cm,

$$t = \left(\frac{(0.09)1076.34}{1e-8} \right) \left[\frac{10}{1076.34} - \ln\left(1 + \frac{10}{1076.34}\right) \right]$$

t = 416067 sec = 5 days.

Similar computations will show that for a depth of 30.5 cms (12 in), the time period is

t = 3822375.82 sec = 44 days.

APPENDIX III

III. Computation of permeability (k_i).

The data sheet corresponding to Chamber A is required for understanding the computation procedure employed. The formula and variables used to compute the relative permeability are given in the data sheet. The subscript "i" is used to denote the area and is 1 for the center, 2 for the middle and 3 for the outer areas

In the data sheet for Chamber A, consider data pertaining to 5/5/04 10:30 PM. "t_{flow} " represents the cumulative time since start of the test, here,

t_{flow} = difference in time from 5/4/04 10:30 AM to 5/5/04 10:30 PM

= 129600 sec = 1.50 days. (Note : 86400 sec = 1 day)

The value of t_{flow} is the x-axis for the plots of relative permeability.

"Δt" denotes the time interval during which the flow of ΣQi was observed. ΣQ1 represents the flow from center observed during a particular time interval Δt. "Δt" varies and has been chosen based on values of flow from particular chambers. The value of "Δt" and "ΣQi", are used for the computation of relative permeability (ki).

For sample computation purpose, consider data pertaining to 5/5/04 10:30 PM, Area 1,

ΣQ_1 = Difference in flow from 5/5/04 10:30 PM to 5/5/04 10:30 AM

= (1000-600) = 400 ml.

Δt = Difference in t_{flow} values corresponding to 5/5/04 10:30 PM and 5/5/04 10:30 AM

= (129600-86400) = 43200 sec.

$$k_i = \frac{(\Sigma Q_i)(L)}{(\Delta t)(p + L - h)(A_i)} \text{.....} cm/\sec.$$

$$k_1 = \frac{(400)(30.5)}{(43200)(985.6 + 30.5 - 10.16)(81.03)}. = 3.46E - 6.....cm/\sec.$$

The value of k_i is plotted along the y-axis in the chart. (Figure 16)

Similar computations have been performed for areas 2 and 3, and values of k_1, k_2 and k_3 are obtained. The k_{Total} is obtained using the formula shown in the data sheet. The same type of computations has been performed for other chambers and the plots are presented in Figures 17 to 21.

Geotechnical Laboratory, Tested by: Ranjan Satyamurthy.
Department of Civil and Environmental Engineering,

Determination of Hydraulic Conductivity (k_i) CHAMBER A PERMEANT = BRINE NO PILE.

Computation of k_i for time interval Δt :

$$k_i = \frac{(\Sigma Q_i)(L)}{(\Delta t)(p + L - h)(A_i)} \text{.....} cm/\text{sec.}`$$

Variables:

Qi = cumulative volume of flow noted from area "i" during cumulative time "t" since start of flow.

t_{flow} = cumulative time since start of flow from chamber.

ΣQ_i = relative volume of flow observed during time Δt.

Δt = time interval during which flow ΣQ_i was measured.

Consider flows recorded during 5/5/04 10:30 AM till 5/5/04 10:30 PM.

ΣQ_1 = 1000 - 600 = 400 ml and Δt = 129600 - 86400 = 43200 sec = 0.5 days.
(Difference in time from 5/5/04 10:30 AM to 5/5/04 10:30 PM)

*The value of k_i is plotted against t_{flow}.

p = pressure head of water entering the chamber (cms) = 14 psi = 985.6 cm of water
(1 psi = 70.4 cm of water)
L = Length of the clay layer = 30.5 cms.
h = pressure head of water discharging from the chamber (cms) (10.16 cm)
Discharge from chambers measured using 3 cylinders of 1000ml capacity (least count 10ml).

A_i = Area of region i in cm^2.

A_1 = Area central annular core = 81.03 cm^2.

A_2 = Area middle annular region = 243.1 cm^2.

A_3 = Area of the outer annular region. = 405.2 cm^2

$A = A_1+A_2+A_3$ = 729.33 cm^2

$$k_{Total} = \frac{(k_1 A_1 + k_2 A_2 + k_3 A_3)}{A}$$

Test Start date: 5/4/04 10:30 AM					**Area 1**		**Area 2**		**Area 3**		**Area 1**	**Area 2**	**Area 3**	**Total Area**
Date & Time	**t_{flow} (sec)**	**t_{flow} (days)**	**Δt (sec)**	**Δt (days)**	**Q_1 (ml)**	**ΣQ_1 (ml)**	**Q_2 (ml)**	**ΣQ_2 (ml)**	**Q_3 (ml)**	**ΣQ_3 (ml)**	**k_1 (cm/sec)**	**k_2 (cm/sec)**	**k_3 (cm/sec)**	**k_{Total} (cm/sec)**
5/5/04 10:30 AM	86400	1.00			600		0		100					
5/5/04 1:30 PM	97200	1.13			700		0		2600					
5/5/04 10:00 PM	127800	1.48			800		0		4600					
5/5/04 10:30 PM	**129600**	**1.50**	**43200**	**0.50**	**1000**	**400**	**0**	**0**	**8600**	**8500**	**3.46E-06**	**0.00E+00**	**1.47E-05**	**8.56E-06**
5/6/04 9:30 AM	169200	1.96			1000		0		12600					
5/6/04 11:00 AM	174600	2.02			1020		0		13700					
5/6/04 1:30 PM	183600	2.13			1620		0		15700					
5/6/04 3:45 PM	191700	2.22			1800		0		16700					

VITA

Ranjan Satyamurthy was born in Mysore, India. He graduated with a Bachelor of Engineering in Civil Engineering from Sri Jayachamarajendra College of Engineering, Visveswaraiah Technological University, India in 2003. His areas of interest are Geotechnical Engineering, Geoenvironmental Engineering, Geosynthetics and related areas. He is an Engineering Intern certified by the Louisiana Professional and Land Surveying Board. He intends to pursue Doctoral studies in Civil and Environmental Engineering at Syracuse University, New York.